Magmatic source and metamorphic grade of metavolcanic rocks from the Granjeno Schist: was northeastern Mexico a part of Pangaea?

ARTICLE *in* GEOLOGICAL JOURNAL · JUNE 2015

Impact Factor: 1.63 · DOI: 10.1002/gj.2702

7 AUTHORS, INCLUDING:

Carita Augustsson
University of Stavanger (UiS)
18 PUBLICATIONS 204 CITATIONS
SEE PROFILE


José Rafael Barboza-Gudiño
Universidad Autónoma de San Luis Potosí
18 PUBLICATIONS 94 CITATIONS
SEE PROFILE

M. Abratis
Friedrich Schiller University Jena
39 PUBLICATIONS 284 CITATIONS
SEE PROFILE


Anders Scherstén
Lund University
91 PUBLICATIONS 985 CITATIONS
SEE PROFILE

GEOLOGICAL JOURNAL
Geol. J. (2015)
Published online in Wiley Online Library
(wileyonlinelibrary.com). DOI: 10.1002/gj.2702

Magmatic source and metamorphic grade of metavolcanic rocks from the Granjeno Schist: was northeastern Mexico a part of Pangaea?

SONIA ALEJANDRA TORRES SÁNCHEZ[1,2]*, CARITA AUGUSTSSON[3], JOSÉ RAFAEL BARBOZA GUDIÑO[4], UWE JENCHEN[1], JUAN ALONSO RAMÍREZ FERNÁNDEZ[1], MICHAEL ABRATIS[2] and ANDERS SCHERSTÉN[5]

[1] *Facultad de Ciencias de la Tierra, Universidad Autónoma de Nuevo León, Linares, Nuevo León, Mexico*
[2] *Institut für Geowissenschaften, Friedrich-Schiller-Universität Jena, Jena, Thüringen, Germany*
[3] *Institutt for Petroleumsteknologi, Universitetet i Stavanger, Stavanger, Norway*
[4] *Instituto de Geología, Universidad Autónoma de San Luis Potosí, San Luis Potosí, Mexico*
[5] *Department of Geology, Lund University, Lund, Sweden*

The geochemistry of the metavolcanic rocks from the Granjeno Schist in northeastern Mexico indicates an origin in different tectonic environments: mid-ocean ridge and ocean island. High ratios of Hf/Th and Th/Nb (4.4–14 and 0.08–0.15), low ratios of LaN/YbN and LaN/SmN (0.74–1.7 and 0.60–1.4) and depleted LREE patterns in metabasalt display mid-ocean ridge characteristics. In contrast, the pattern of trace-element ratios and REEs in metabasalt and metapillow lava 60 km to the west indicates a magma source with ocean-island basalt characteristics. Both areas were metamorphosed during the Late Carboniferous (300 ± 4 Ma). Estimated metamorphic conditions deduced from white mica and chlorite compositions, distinguish greenschist facies (350 °C and 4 kbar) for the mid-ocean ridge basalt, and prehnite–pumpellyite facies (250 °C and 2.5 kbar) for the ocean-island-type basalt. This metamorphism took place at an active continental margin during Pennsylvanian time. Our new tectonic model, which differs from earlier models, suggests that the origin of the Granjeno Schist is related to a subduction zone located at the western margin of Pangaea, active after Laurentia–Gondwana collision.

Received 21 October 2014; accepted 18 May 2015

KEY WORDS Granjeno Schist; northeastern Mexico; Gondwana; Rheic Ocean; Pangea; Late Carboniferous

1. INTRODUCTION

Gondwana collided with Laurentia to form Pangaea between *ca*. 320 and 300 Ma (Cawood *et al*., 2009). During the interval of approach and collision, several small terranes were separated from Gondwana and accreted to Laurentia (Ziegler, 1990; Stampfli and Borel, 2002; Blakey, 2007). One of these small terranes was Oaxaquia, which consists of Grenville-age granulite-facies rocks. These rocks are distributed throughout northeastern, central and southern Mexico (Ortega-Gutiérrez *et al*., 1995). The Oaxaquia terrane underlies most of the Mexican mainland and possibly extends beneath Honduras; the total area including the suggested extension is at least 10^6 km^2 (Cameron *et al*., 2004). Several authors (e.g. Ortega-Gutiérrez *et al*., 1995; Keppie and Ortega-Gutiérrez, 1995, 1999) have proposed that Oaxaquia is a microcontinent.

Outcrops of Grenville-age rocks comprising Oaxaquia occur from northeastern to southern Mexico (Fig. 1a). Specific occurrences include (a) the Novillo Gneiss, Tamaulipas; (b) lower crustal xenoliths, central Mexico; (c) the Huiznopala Gneiss, Hidalgo; (d) the Oaxacan Complex and the Guichicovi Gneiss, Oaxaca; and (e) in the Chiapas Massif, Chiapas (Fries *et al*., 1962; Fries and Rincón-Orta, 1965; Murillo-Muñetón *et al*., 1994; Ortega-Gutiérrez, 1978; Ortega-Gutiérrez, 1984; Pantoja-Alor *et al*., 1974; Patchett and Ruiz, 1987; Ruiz *et al*., 1988, Yañez *et al*., 1991; Silver *et al*., 1994).

Vestiges from the late Palaeozoic collision between Laurentia and Gondwana are scarce but not absent in Mexico. Visible remnants include the Palaeozoic rocks of the Granjeno Schist in northeastern Mexico and in the southern Acatlán Complex (Fig. 1a; Nance *et al*., 2007). These rocks have an Oaxaquia inheritance (Stewart *et al*.,

*Correspondence to: S. A. Torres Sanchez, Facultad de Ciencias de la Tierra, Universidad Autonoma de Nuevo Leon, Hacienda de Guadalupe, Carretera a Cerro Prieto, km 8 Linares Nuevo Leon 67700, Mexico. E-mail: soniatorressan@hotmail.com

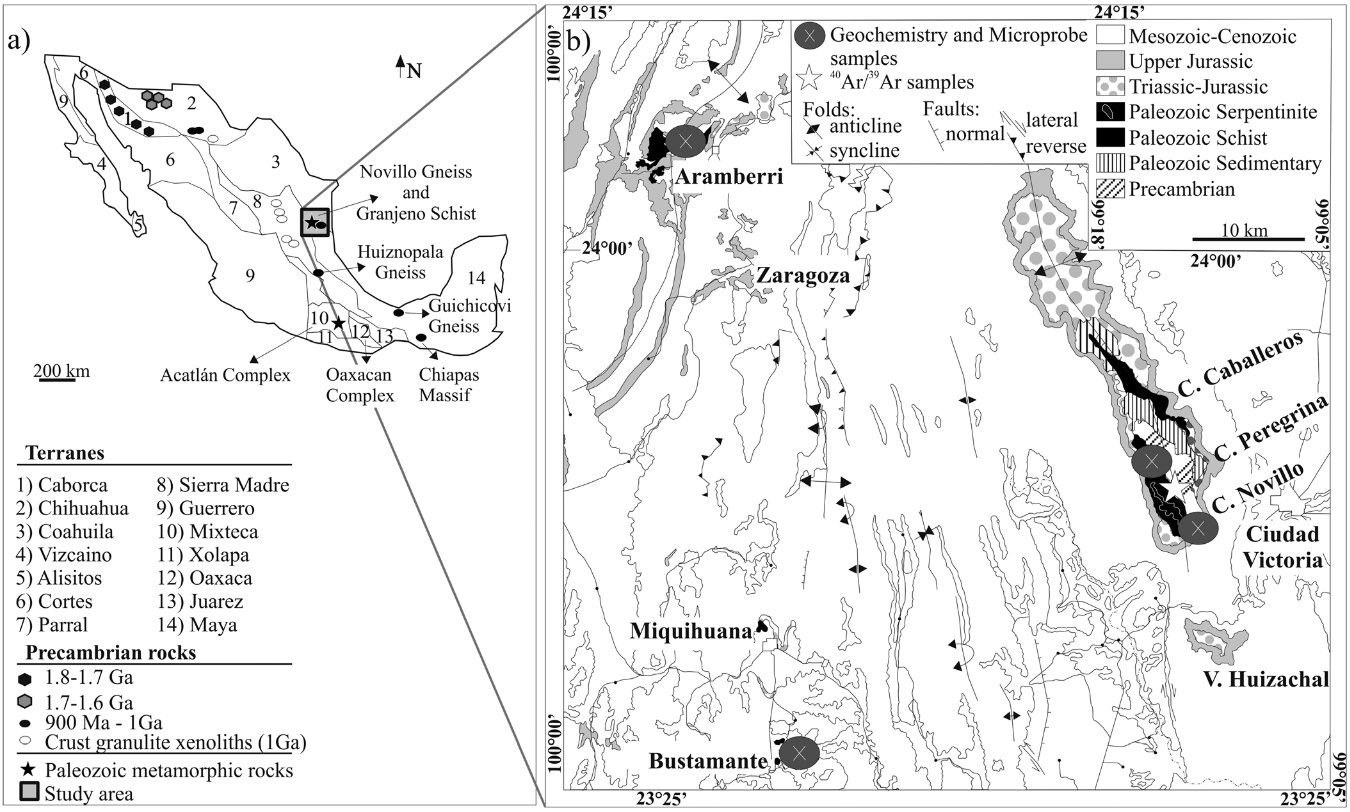

Figure 1. (**a**) Precambrian and Palaeozoic metamorphic rocks in Mexico. Modified from Campa and Coney (1983) and Ortega-Gutiérrez *et al.* (1995) and (**b**) study area (after Barboza-Gudiño *et al.*, 2011) with the Granjeno Schist.

1999) and are remnants of the Palaeozoic Rheic Ocean (Keppie and Ramos, 1999; Nance *et al.*, 2010). The closure of this ocean was accompanied by the >10 000 km Variscan–Alleghanian–Ouachita Orogeny within the assembled Pangaea supercontinent (Nance and Linnemann, 2008).

In Mexico, details of the Laurentia–Gondwana collision remain controversial (Mickus and Montana, 1999). Even though several studies have examined the Palaeozoic of northeastern Mexico (Carrillo-Bravo, 1961; De Cserna and Ortega-Gutiérrez, 1977; Ramírez-Ramírez, 1978, 1992; Cossío Torres, 1988; Torres-Sánchez *et al.*, 2013; Castillo-Rodríguez, 1988; Orozco-Esquivel, 1991; Ortega-Gutiérrez *et al.*, 1995; Ehricke, 1998), the development of the Palaeozoic (Silurian to Carboniferous) basement rocks has received less attention (Keppie and Ramos, 1999; Dowe *et al.*, 2005; Nance *et al.*, 2007, 2009, 2010; Nance and Linnemann, 2008; Torres-Sánchez, 2010; Barboza-Gudiño *et al.*, 2011). The origin and evolution of the Silurian and Carboniferous units, which are part of the Palaeozoic basement in northeastern Mexico, are not completely understood. It is commonly accepted that the Granjeno Schist metamorphism was related to the closure of the Rheic Ocean and the resulting formation of Pangaea. Those ideas were based on field relationships and petrographic and isotopic characterization of metasedimentary rocks only (Keppie and Ramos, 1999; Keppie, 2004; Dowe *et al.*, 2005; Nance *et al.*, 2007, 2010; Nance and Linnemann, 2008). No particular attention has been given to the metavolcanic rocks of the Granjeno Schist. Hence, until now, the relation between the protoliths of the metasedimentary and the metavolcanic rocks and the plate-tectonic setting has not been considered for plate-tectonic reconstructions and the implication for the northwestern Gondwana evolution.

Since the 1970s, the metavolcanic rocks from the Novillo Canyon have been reported to have an oceanic affinity, but only field studies were used as evidence (Ramírez-Ramírez, 1974, 1978, 1992; De Cserna and Ortega-Gutiérrez, 1977, 1978; Ortega-Gutiérrez, 1978). This study is the first to address the petrology and geochemistry of Palaeozoic metavolcanic rocks in northeastern Mexico. The purposes of the study are (a) to establish the tectonic setting of the volcanic protoliths as accurately as possible, (b) to determine the metamorphic age and metamorphic conditions that affected these rocks, (c) to establish a geological model for the evolution of Palaeozoic magmatism in northeastern Mexico, and (d) to relate it to the evolution of Pangaea. In order to achieve this, we use primary and secondary mineralogical compositions, mineral and whole-rock chemistry as well as metamorphic $^{40}Ar/^{39}Ar$ ages of the metavolcanic rocks of the Granjeno Schist.

2. GEOLOGIC SETTING

The Granjeno Schist is a polydeformed sequence that includes both sedimentary (psammite, pelite, turbidite, conglomerate and black shale) and igneous (tuff, lava flows, pillow lava and ultramafic bodies) protoliths that have been metamorphosed under subgreenschist to greenschist facies conditions (Carrillo-Bravo, 1961; De Cserna and Ortega-Gutiérrez, 1978; Ramírez-Ramírez, 1974, 1992; Dowe *et al*., 2005; Torres-Sánchez, 2010). The Granjeno Schist crops out in axes of anticlines in the Sierra Madre Oriental in northeastern Mexico, for example, in the Huizachal–Peregrina anticlinorium. This N-NW-trending, double-plunging structure is located northwest of Ciudad Victoria in Tamaulipas (Fig. 1b; Zhou *et al*., 2006). A major NW–SE-trending dextral fault separates the Granjeno Schist from the Mesoproterozoic Novillo Gneiss in this locality. A body of plagiogranite (Ramírez–Ramírez, 1992) with an intrusion age of 351 ± 54 Ma (U-Pb in zircon) and a cooling age of 313 ± 7 Ma ($^{40}Ar/^{39}Ar$ in muscovite; Dowe *et al*., 2005) is located in the fault contact.

Isolated outcrops of the Granjeno Schist are present in the Miquihuana and Bustamante Uplift (Tamaulipas) areas southwest of the Huizachal–Peregrina anticlinorium (Fig. 1b). In these areas, the Granjeno Schist is unconformably overlain by Early–Middle Jurassic volcanic rocks and redbeds. The Granjeno Schist also crops out in the Aramberri Uplift, Nuevo Leon (Fig. 1b), where it is overlain by Early Jurassic volcanic rocks, Early–Middle Jurassic redbeds, Late Jurassic breccia and Late Jurassic evaporite and carbonate rocks (Imlay, 1938; Heim, 1940; Humphrey, 1954; Mixon *et al*., 1959; Barboza-Gudiño *et al*., 2008).

The metamorphic age of the metasedimentary rocks of the Huizachal–Peregrina anticlinorium has been investigated in several studies. Most recently, Dowe *et al*. (2005) reported a $^{40}Ar/^{39}Ar$ plateau age on phengite of 300 ± 4 Ma from the Novillo Canyon. Older Rb-Sr whole-rock muscovite isochron ages range from 318 ± 10 Ma to 257 ± 8 Ma (Fries *et al*., 1962; De Cserna and Ortega-Gutiérrez, 1977). Whole-rock Rb-Sr ages of 373 ± 37 Ma to 320 ± 12 Ma are recalculated from De Cserna and Ortega-Gutiérrez (1978), Garrison *et al*. (1980) and Sedlock *et al*. (1993). The metasedimentary rocks from the Aramberri Uplift yield muscovite K-Ar ages from 270 ± 5 to 294 ± 6 Ma (Denison *et al*., 1971). This paper provides the first metamorphic ages of the metavolcanic rocks from the Granjeno Schist.

3. SAMPLING AND ANALYTICAL METHODS

Fifteen samples from the Granjeno Schist, consisting of massive metabasalt, metabasaltic flows and metapillow lava were analysed for mineral–chemical composition and major and trace element contents and $^{40}Ar/^{39}Ar$ isotopic composition. Six samples were collected from the Aramberri Uplift, three from the Bustamante Uplift, one from Novillo Canyon and five from Peregrina Canyon. Petrographic analyses were first accomplished for all 15 samples with a polarizing microscope (Table 1).

Chemical compositions of minerals were analysed with the electron microprobe JEOL JXA 8230 at the Institute of Geosciences of the Friedrich-Schiller University, Jena, Germany. Chlorite, amphibole, clinozoisite, zoisite, feldspar, mica, pumpellyite, pyroxene and prehnite compositions

Table 1. Coordinates, lithology, mineral content and methods of the studied metavolcanic rocks from the Granjeno Schist

Sample	Location	Coordinates (WGS 84)	Lithology	Mineralogy	Method
A12a	AU	140410132E, 2667106 N	Metapillow	Chl + Plg + Ac + Qz + Cal	MP
A44	AU	140410132E, 2667106 N	Massive metabasalt	Chl + Plg + Qz + Cal	GC
A58A	AU	140410230E, 2667130 N	Metapillow	Ab + Chl + Pmp + Cal	GC
A58B	AU	140410230E, 2667130 N	Metapillow	Ab + Chl + Cal	GC
A58D	AU	140410230E, 2667130 N	Metapillow	Ab + Chl + Cal	GC
B1	AU	Sample from private company	Massive metabasalt	Chl + Ta + Px + Ab + Ac + Pmp	MP
Bu1	BU	140424088E, 2593846 N	Metabasaltic flow	Cpx + Zo + Ag ti + Am + Prh + Pmp	MP
Bu11	BU	140423974E, 2593867 N	Massive metabasalt	Cpx + Czo + Plg + Pmp + Chl	GC
Bu11b	BU	140423974E, 2593867 N	Massive metabasalt	Cpx + Czo + Plg + Pmp + Chl	GC
CNS11	NC	140472256E, 2623140 N	Massive metabasalt	Czo + Chl + Cpx + Prh + Pmp + Ab + Am	GC, MP
CPS8	PC	140470007E, 2627535 N	Metabasaltic flow	Chl + Ab + Cal + Czo + Cpx + Mu + Zo + Zr	GC
CPS9	PC	140469830E, 2627335 N	Metabasaltic flow	Prh + Ab + Czo + Cal + Qz + Cpx	GC
CPS10	PC	140469664E, 2627327 N	Metabasaltic flow	Zo + Czo + Px + Chl + Qz + Plg + Pmp	MP
CPS11	PC	140469467E, 2627303 N	Metabasaltic flow	Zo + Czo + Mu + Pmp	GC, G
CPS13	PC	140469291E, 2627354 N	Metabasaltic flow	Ab + Chl + Qz + Mu + Zo + Czo + Ac	MP

Ab, albite; Ag ti, titaniferous augite; Ac, actinolite; Am, amphibole; Cal, calcite; Chl, chlorite; Cpx, clinopyroxene; Px, pyroxene; Plg, plagioclase; Pmp, pumpellyite; Prh, prehnite; Qz, quartz; Ta, talc; Zo, zoisite; Czo, clinozoisite; AU, Aramberri Uplift; BU, Bustamante Uplift; NC, Novillo Canyon; PC, Peregrina Canyon; MP, Microprobe analysis; GC, geochemical analysis; G, Geochronological analysis.

DOI: 10.1002/gj

(Appendices 1–8, see Supporting Information) were determined from samples of all four study areas. The microprobe excitation voltage was 15.0 kV, and the beam current was 15 nA. A beam size of 2–3 μm (10 μm for albite analysis) was used. All standards were certified silicates and oxides.

Total abundances of major oxides and trace elements were measured for ten samples: three metapillow lava, four massive metabasalt and three metabasaltic flow samples (Table 1). They were powdered in an agate mill and analysed with ICP-OES (major element oxides) and ICP-MS/INAA (Cs, Sr, Ba, Th, Co, Hf, Ta and REE) with an accuracy of ±5–20% at ACTLABS (Ancaster, Ontario, Canada). We used the molecular proportions of Al_2O_3, MgO, K_2O, Na_2O and CaO to calculate the Numerical Index of Alteration (AI = [100]*[[MgO + K_2O]/[MgO + K_2O + CaO + Na_2O]]), the Chemical Index of Alteration (CIA = [100]* [[Al_2O_3]/[Al_2O_3 + CaO + Na_2O + K_2O]]) and the Plagioclase Index of Alteration (PIA = [100]*[[Al_2O_3-K_2O]/[Al_2O_3 + CaO + Na_2O-K_2O]]) of Ishikawa *et al.* (1976) and Nesbitt and Young (1982) in order to evaluate the major-element mobility from the total abundance estimations. To resolve the tectonic setting in which the basaltic lavas extruded, the composition of immobile trace elements was examined and is presented here with two characteristic ternary and three simple bivariate traditional tectonomagmatic discrimination diagrams (Zr/4-Y-2Nb of Meschede, 1986; Th-Nb/16-Hf/3 of Wood, 1980; Ti/1000-V of Shervais, 1982; (La/Sm)n-Δ Nb and Zr/Y-Nb/Y of Fitton *et al.*, 1997, 2003). The obtained results were compared with multi-dimensional discrimination diagrams that were successfully applied for inferring the tectonic setting of metamorphosed or altered basalt (Agrawal *et al.*, 2008; Verma and Agrawal, 2011).

In preparation to create multi-dimensional discrimination diagrams, we adjusted the major-element oxide data (ADJ) using the programme 'Igneous Rock Classification System' (IgRoCS; Verma and Rivera-Gómez, 2013a). Adjusted data were further computed using the programme TecD (Tectonomagmatic Discrimination) from Verma and Rivera-Gómez (2013b), which evaluates igneous rock geochemistry data in 20 different multi-dimensional diagrams. The diagrams are based on natural logarithms of element ratios (e.g. In (TiO_2/SiO_2)) and linear discriminant analysis as elaborated by Verma and co-workers. The multi-dimensional diagrams are suitable to illustrate different tectonic groups (i.e. island arc, continental rift, ocean island and mid-ocean ridge) in data plots. These diagrams are based on abundances of major elements and the immobile elements La, Sm, Yb, Nb, Th, Nb, V, Y and Zr (Verma *et al.*, 2012, 2013; Verma, 2013; Verma and Verma, 2013; Armstrong-Altrin, 2015).

The metamorphic age of metabasalt CPS11 from Peregrina Canyon was dated with the Ar–Ar method. Muscovite crystals were pretreated to remove possible traces of weathered material, separated by standard techniques and selected by handpicking under a binocular microscope from the 50–100 μm size fraction. Ar was measured from three aliquots of a muscovite concentrate of the same groundmass. We used laser step-heating techniques and a Micromass 5400 mass spectrometer with a Faraday multiplier and an electron multiplier at the Geochronology Laboratory, Lund University, Sweden. The sample, which was loaded into a copper planchette that contains several 3 mm holes, was step-heated using a defocused 50 W CO_2-laser. Rastering the laser beam over the sample provided uniform heating of all grains. An automated analytical process runs on a Macintosh OS 10.2 platform with software customized for the Lund laboratory. Regressions to time zero were fitted to data collected from ten scans over the mass range of 36 to 40. Peak heights and backgrounds were corrected for mass discrimination, isotope decay and interfering nucleogenic Ca-, K- and Cl-derived isotopes. Sanidine standard TCR (t = 28.34 Ma, Renne *et al.*, 1998) was used, and J values were calibrated with a precision of ±0.25%. The samples were irradiated at the Petten reactor. A step-heating age spectrum plot displays a plateau age interpreted to be meaningful when the apparent age for at least three consecutive steps comprises a minimum of 50% of the total released ^{39}Ar (Dickin, 2005). Isoplot 4.15 software (Ludwig, 2012) was used to calculate a weighted mean age and 2σ errors.

Metamorphic temperatures for the metavolcanic rocks were determined using the chlorite thermometer of Cathelineau (1988), which is based on Al^{IV} in chlorite, and compared with the corrected thermometer by Jowett (1991). The temperature calculation considers the influence of iron in chlorite and requires that Fe/(Fe + Mg) to be <0.6. Pressures were estimated by the phengite geobarometer of Velde (1965) and Massonne and Schreyer (1987). Appendices 1–9 and 11 (see Supporting Information) provide mineral and whole-rock chemical compositions, ^{40}Ar/^{39}Ar data and a list of compositional preconditions for the calculated metamorphic conditions.

4. RESULTS

4.1. Macroscopic description of the metavolcanic rocks in the Granjeno Schist

The metavolcanic rocks of the Huizachal–Peregrina anticlinorium crop out in the Peregrina and Novillo Canyons as metatuff and metabasalt, and in the Aramberri–Bustamante Uplifts as metatuff, metabasalt and metapillow lava.

The metatuff at the Peregrina and Novillo Canyons consists of fine-grained, homogeneous, greenish to bluish lustrous layers with NW–SE-trending foliation, ranging in thickness from 1 cm to 20 m, and rhythmically interbedded with metapelite and metapsammite (Fig. 2a).

DOI: 10.1002/gj

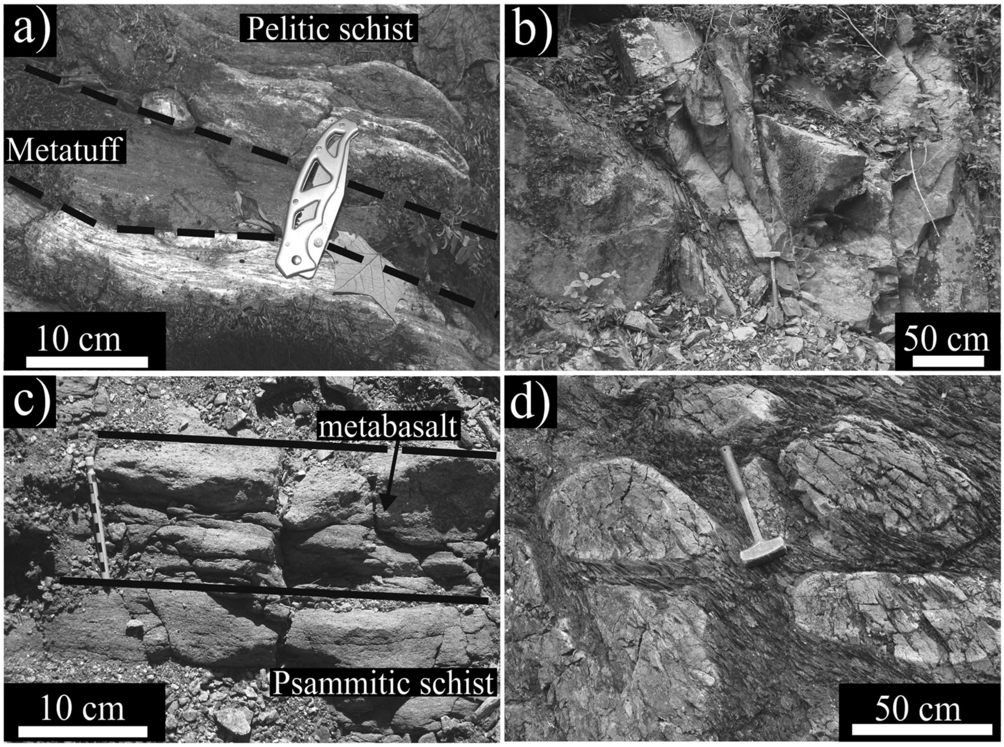

Figure 2. (**a**) Interbedded metatuff from the Novillo Canyon, (**b**) fractured metabasalt flow in the Peregrina Canyon, (**c**) microcrystalline metabasalt flow at the Peregrina Canyon and (**d**) metapillow lava in the Aramberri Uplift.

Two types of metabasalt can be distinguished. Massive metabasalt in the Novillo Canyon is greenish to greyish, coarse-crystalline, fractured and with weakly developed foliation (Fig. 2b). It lacks flow structures and occurs in fault-parallel contact to the main foliation of the metasedimentary rocks. Fine-crystalline metamorphosed basalt flows with internal flow structures in the Peregrina Canyon, occur as packages up to 2 m thick whose contacts are concordant with metasedimentary rocks (Fig. 2c).

The metatuff at Bustamante Uplift occurs as 2-cm- to 1-m-thick layers interbedded with metapelite. A rhyolitic dyke cuts the metapelitic sequence perpendicularly.

Metapillow lava at Aramberri Uplift occurs as lithosomes of coarse-grained greenish rocks intercalated with metasedimentary layers in packages of 2–5 m thickness. Pillow structures are well preserved (Fig. 2d). Black and dark green zones are dominated by chlorite–pumpellyite, and light green zones by epidote.

4.2. Petrographic composition

The meta-igneous rocks are mainly composed of the metamorphic minerals chlorite, white mica, prehnite, pumpellyite, clinozoisite, zoisite, feldspar and amphibole. Relict clinopyroxene is recognizable.

In the metapillow lava, metaporphyritic and meta-ophitic textures predominate. Relict diopside is partially altered to chlorite. It is present in polymineralic quench crystallites of albitized plagioclase (Fig. 3a). The groundmass has a low abundance of hypidiomorphic microcrystals (e.g. quartz, epidote, actinolite and calcite, ≤0.33 mm). The diameters of amygdules range from 0.5 to 2.5 mm. Their original structures have been replaced by metamorphic minerals. The amygdules are filled with albite (Ab_{99}), quartz and pumpellyite or alternatively with albite, quartz and chlorite (pychnochlorite type; Fig. 3b).

The massive metabasalt has both meta-ophitic and porphyroblastic textures. Three common types of porphyroblasts are recognized: (1) subhedral albite with Ab_{99} composition (0.5 to 2 mm; Fig. 3c), (2) fractured subhedral diopside from 0.5 to 2 mm (Fig. 3d) and (3) tabular clinozoisite up to 0.5 mm (Fig. 3e). All porphyroblast types are surrounded by acicular pumpellyite and chlorite (ripidolite) up to 0.5 mm in a subhedral prehnite groundmass. Calcite is present as a secondary mineral.

The metabasaltic flow has a porphyrolepidoblastic texture with elongated and subhedral, 2.0–3.5 mm-sized zoisite–clinozoisite and up to 2-mm-sized subhedral albite porphyroblasts. Discontinuously zoned clinozoisite with an iron-rich core is common (Fig. 3e–f). The zoisite has anomalous blue interference colours. The porphyroblasts are in a fine

DOI: 10.1002/gj

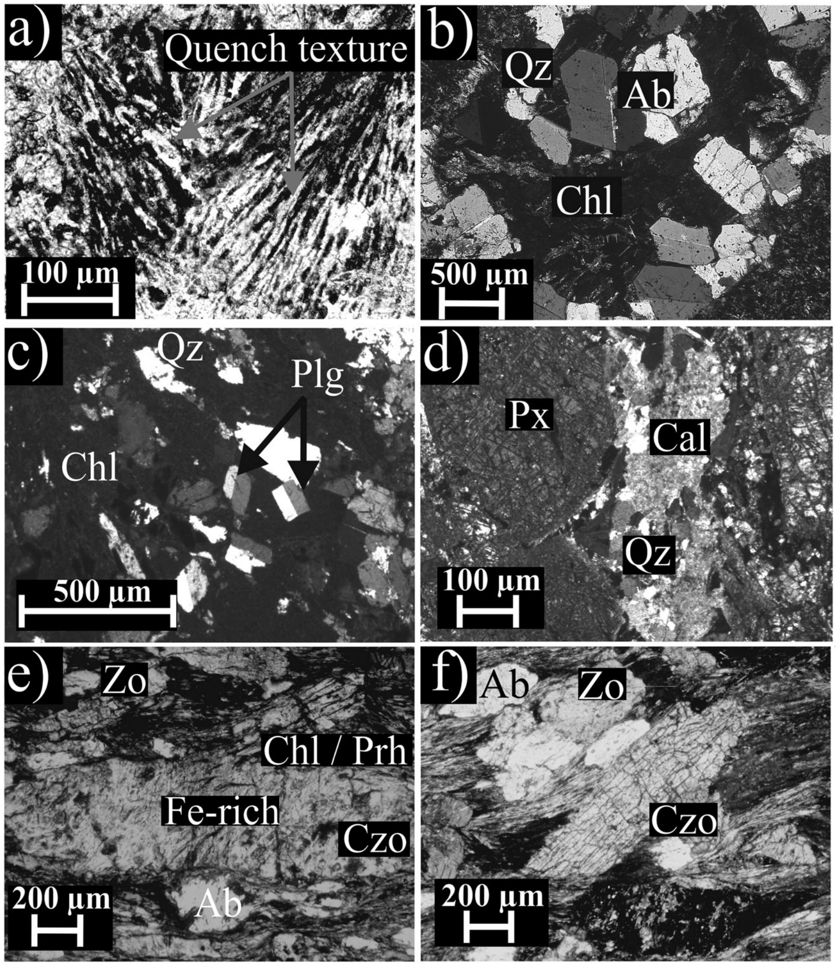

Figure 3. Representative photomicrographs of the metaigneous rocks. (**a**) Plane-polarized light image with relic acicular quench texture in metapillow lava (A58b), (**b**) amygdule filled with albite, quartz and chlorite in metapillow lava (crossed polars; A12a), (**c**) metabasalt with phenocrysts of tabular plagioclase and subhedral quartz in a chlorite groundmass (crossed polars; A44), (**d**) metabasalt with porphyroblastic texture dominated by fractured subhedral clinopyroxene porphyroblasts. Calcite and quartz are present as secondary minerals (crossed polars; Bu11), (**e–f**) subhedral clinozoisite-zoisite with iron-rich core (crossed polars, CPS10). Ab, albite; Cal, calcite; Chl, chlorite; Czo, clinozoisite; Px, pyroxene; Plg, plagioclase; Prh, prehnite; Qz, quartz; Zo, zoisite.

pumpellyite groundmass and surrounded by *ca*. 0.5-mm-long fibrous prehnite and chlorite (clinochlore and pycnochlorite).

4.3. Mineral–chemical composition

4.3.1. Relict pyroxene

Relict clinopyroxene occurs as fractured, hypidiomorphic, granular and colourless crystals (Fig. 4a). The clinopyroxene in the massive metabasalt and metabasaltic flow from the Aramberri and Bustamante Uplift areas has a limited compositional range (diopside: $Wo_{45\text{-}50}En_{43\text{-}50}Fs_{5–15}$) (Appendix 1, see Supporting Information). The diopside contains 0.95–3.17% TiO_2, 0.28–0.56% Na_2O and 44–51% SiO_2 (Fig. 5).

4.3.2. Metamorphic minerals

4.3.2.1. Chlorite. Chlorite, the most common mineral in the metavolcanic rocks, occurs as tabular crystals in fine-grained groundmass, irregular interstitial patches inside plagioclase and filling of amygdules (Fig. 4b). It has been formed from both alteration of volcanic glass and as a replacement product of igneous pyroxene and olivine. All chlorite is dark yellow to green, displaying brown anomalous birefringence. Violet/blue birefringence characterizes chlorite filling amygdules in metapillow lava and interstitial patches in the massive metabasalt.

Brown chlorite in the metabasaltic flow of the Bustamante Uplift and Peregrina Canyon has Fe/(Fe + Mg) ratio of 0.4–0.5 and Al_{tot} values of 2.1–2.6 atoms per formula unit (apfu). Brown and violet/blue chlorite in the metapillow lava of the Aramberri Uplift and in the massive metabasalt of Novillo Canyon has Fe/(Fe + Mg) ratio of 0.3–0.4 and Al_{tot} values of 1.4–2.6 apfu. Thus, birefringence colours depend principally upon Al_{tot}. These compositions, together with Si = 2.7–3.7 apfu, classify the chlorite as ripidolite. Higher Si (3.0–3.8 apfu) for metapillow chlorite at Aramberri Uplift

DOI: 10.1002/gj

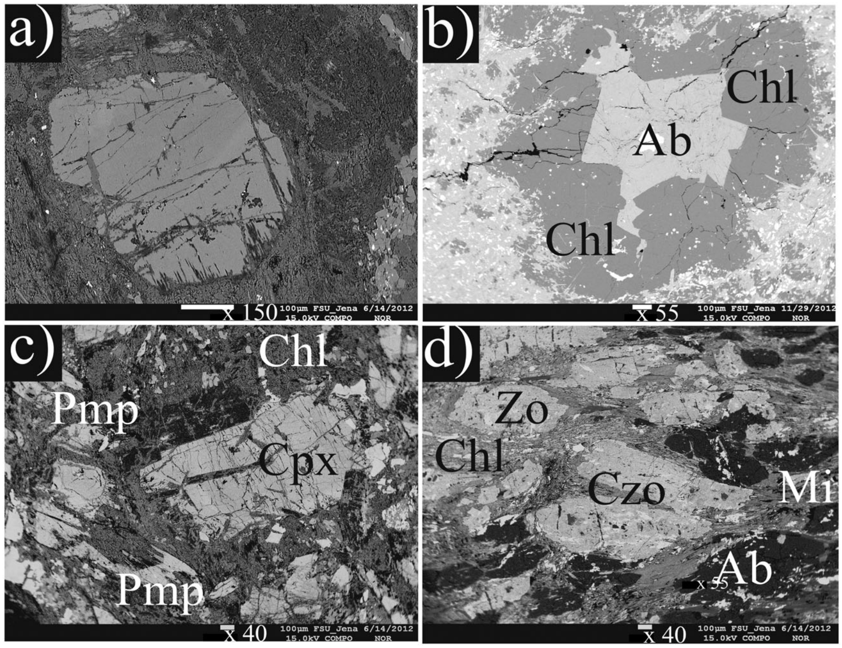

Figure 4. Backscattered electron images of metavolcanic rocks. (**a**) Diopside from massive metabasalt (sample B1), (**b**) chlorite as interstitial patches inside plagioclase in metapillow lava (sample A12a), (**c**) xenomorphic pumpellyite in basaltic flow (Sample Bu1) and (**d**) zoisite and clinozoisite porphyroblasts in basaltic flow (sample CPS10). Cpx, clinopyroxene; Pmp, pumpellyite; Mi, mica. For further abbreviations, see Fig. 3.

classify the mineral as pycnochlorite (Fig. 6a and Appendix 2 (see Supporting Information)).

4.3.2.2. Chlorite geothermometer. The tetrahedral Al (Al^{IV}) content in chlorite is 0.71–1.07 apfu for the metapillow lava and flows of the Aramberri and Bustamante Uplifts. This is in accordance with crystallization temperatures of 165–276 °C (Appendix 2, see Supporting Information; cf. Cathelineau, 1988). Mean temperatures are 216 °C ($n = 2$; with a temperature difference of 101 °C) for the Bustamante Uplift and 235 °C ($n = 7$; largest difference: 46 °C) for the Aramberri Uplift. The massive metabasalt and flows from the Novillo and Peregrina Canyons yield Al^{IV} contents of 1.21–1.31 apfu, and correspondingly higher temperatures of 328–360 °C with mean values of 346 °C ($n = 6$; largest difference: 32 °C) and 349 °C ($n = 2$; difference: 1 °C), respectively. All analysed chlorite has Fe/(Fe + Mg) ratios of <0.6, which is taken into account for temperature calculations according to Jowett (1991). This gives temperatures that are 40–60 °C higher than the mean temperatures derived from the Cathelineau (1988) thermometer (Appendix 2, see Supporting Information).

4.3.2.3. Pumpellyite. Scarce pumpellyite is associated with albite, clinozoisite, zoisite, chlorite, amphibole and prehnite (Fig. 4c). Pumpellyite occurs as colourless prismatic crystals in amygdules, as yellowish acicular and radial crystals in the groundmass and as brown xenomorphic crystals in rims of plagioclase and pyroxene. Fe/(Fe + Al) is a uniform 0.15 in iron-rich pumpellyite, whereas aluminium-rich pumpellyite from the metabasaltic flow of the Bustamante Uplift has an Fe/(Fe + Al) ratio of 0.02. In the massive metabasalt of the Aramberri Uplift and Novillo Canyon, the MgO/(MgO + FeO) ratio is 0.1–0.2 and 0.92 in the metabasaltic flow of the Bustamante Uplift (Appendix 3, see Supporting Information).

4.3.2.4. Zoisite and clinozoisite. Epidote-group minerals occur as fractured hypidiomorphic and prismatic porphyroblasts associated with pumpellyite, actinolite, chlorite, albite and quartz (Fig. 4d). In general, unzoned epidote-group minerals with anomalous blue interference colour are iron-poor with $Fe^{3+}/(Fe^{3+}+Al) = 0.06–0.25$ (Appendix 4, see Supporting Information).

4.3.2.5. Amphibole. Ubiquitous amphibole is present as uncoloured, greenish and brownish phenocrysts, as fibrous minerals in the groundmass and as replacement of relict clinopyroxene. The amphibole is associated with chlorite, white mica, epidote, pumpellyite, quartz and albite. Amphibole-chemical composition is calcic (Appendix 5, see Supporting Information), dominated by actinolite with <2% Al_2O_3. The $Mg/(Mg + Fe^{2+})$ ratio for actinolite–chlorite coexisting pairs ranges between 1.7 and 2.0. These values are comparable with a low-grade metamorphic origin (cf. Coombs *et al.*, 1976).

4.3.2.6. Mica. White potassic mica is present in minor proportions in all studied rocks. It occurs as tabular crystals, as small flakes in amygdules, and in veins and preferably in

DOI: 10.1002/gj

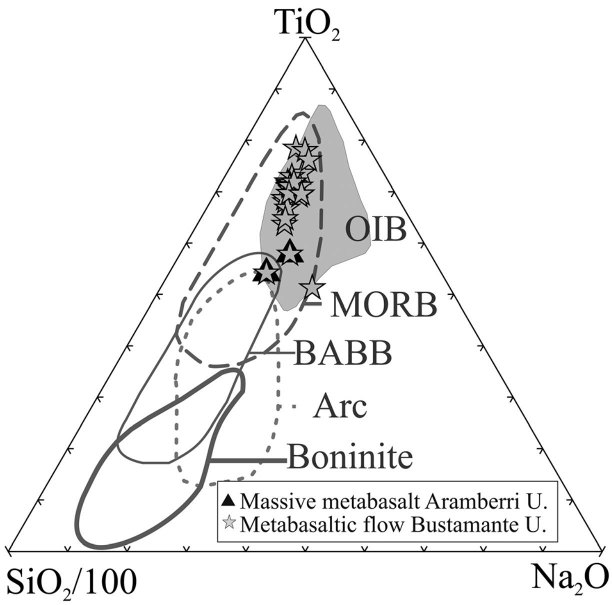

Figure 5. TiO_2-Na_2O-SiO_2/100 (wt%) for discrimination of clinopyroxene from basalt from different tectonic settings according to Beccaluva *et al.* (1989). MORB, mid-ocean ridge basalt; OIB, ocean-island basalt; BABB, back-arc basin basalt.

contact with plagioclase phenocrysts (Fig. 4d). The analysed muscovite is mainly phengitic with Si/Al ratios in the tetrahedral site higher than 3:1 and with a Si content of 3.4 (11 O per formula unit). Na_2O and TiO_2 were detected with <0.15 apfu (Appendix 6, see Supporting Information). This is comparable to phengite of pumpellyite–actinolite facies. The cationic ratios $a = {}^{VI}R^{2+}/({}^{VI}R^{2+} + {}^{VI}R^{3+})$ and $b = {}^{VI}Al/({}^{VI}Al + {}^{VI}Fe^{3+})$ are 0.31 to 0.36 and 0.84 to 0.88, respectively, in the massive metabasalt of the Aramberri Uplift and 0.21 to 0.24 and 0.83 to 0.92, respectively, in the metabasaltic flows of the Bustamante Uplift and Peregrina Canyon. These values correspond to phengitic aluminoceladonite and phengite (Fig. 6b; Kawachi, 1975; Coombs *et al.*, 1976; Guidotti and Sassi, 1998). The cationic ratios of phengitic aluminoceladonite are comparable with subgreenschist facies, whereas the cationic ratios of phengite are similar to greenschist facies (cf. Wise and Eugster, 1974).

4.3.2.7. Feldspar. Plagioclase is homogeneous albite (Ab_{99}, Appendix 7, see Supporting Information). Incompletely albitized plagioclase is absent.

4.3.2.8. Prehnite. Rare prehnite occurs in Novillo massive metabasalt CNS11 and in Bustamante metabasalt flow Bu1. Prehnite is colourless to yellow, showing irregular, radial crystals of low relief. It is presently associated with patches of plagioclase and quartz, filling amygdules and veins and dispersed in the groundmass. Prehnite from the massive Novillo metabasalt is enriched in iron: Fe/(Fe + Al) = 0.19 (Appendix 8, see Supporting Information), but in the Bustamante metabasaltic flow, the ratio is only 0.05 (Appendix 8, see Supporting Information).

5. WHOLE-ROCK GEOCHEMICAL COMPOSITION

5.1. Major- and trace-element composition

In a total alkali-silica classification, whole rocks have a basaltic composition (SiO_2 = 40 to 50 wt%, $Na_2O + K_2O$ <5 wt%). The loss on ignition ranges from 4.4% to 11.3%. The major

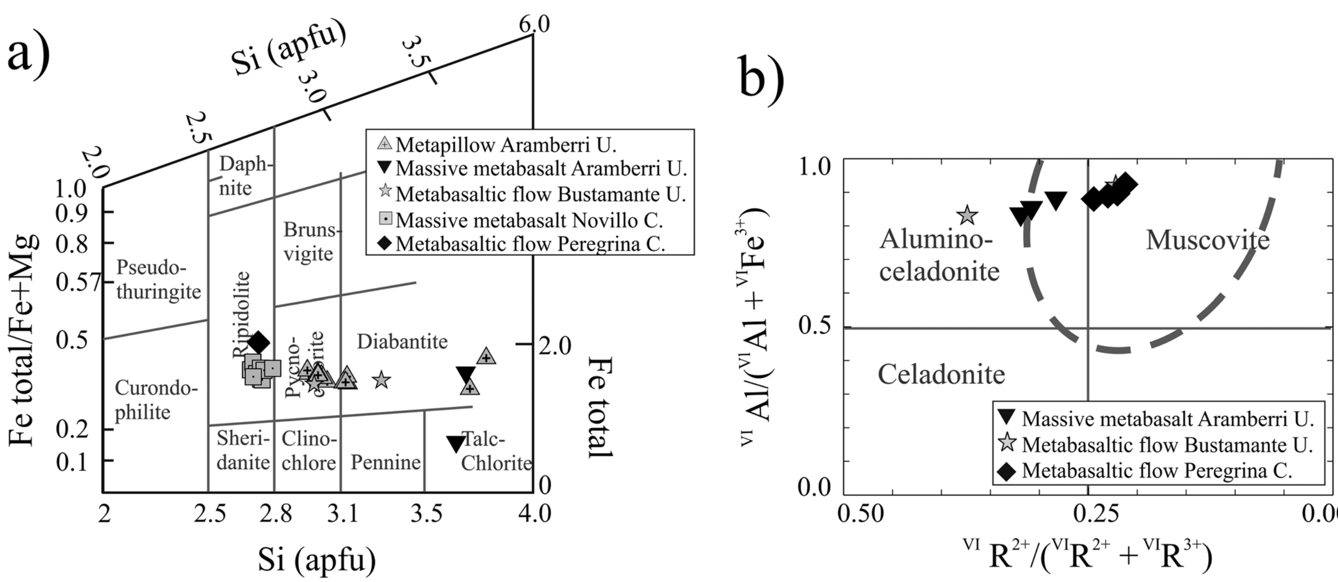

Figure 6. (**a**) Si versus Fe total/(Fe + Mg) (apfu) for chlorite according to Hey (1954). (**b**) Mica classification scheme based on Guidotti and Sassi (1998). The dashed line marks a field that represents the compositional range of the phengite series. ${}^{VI}R^{2+} = Mg + Fe^{2+} + Mn$; ${}^{VI}R^{3+} = Al + Fe^{3+}$; ${}^{VI}Al$: octahedral aluminium and ${}^{VI}Fe^{3+}$ = octahedral iron.

element mobility estimated by the Numerical Index of Alteration ranges from 45 to 96. These values match well with the low ratios of the Chemical Index of Alteration of 25–63 and the Plagioclase Index of Alteration of 25–64. The elements La, Sm, Th, Nb, Hf and Ti exhibit a good correlation with the immobile trace element Zr ($r \geq 0.85$), whereas incompatible elements K, Sr, Ba and Rb of the analysed rocks are widely scattered ($r < 0.85$).

The Mg# is primitive: 48–67 (Appendix 9, see Supporting Information). TiO_2% in Bustamante and Aramberri metapillow lava and massive metabasalt is relatively high with 2.4 to 3.3 wt%, but 1.5 to 1.8 wt% in Peregrina and Novillo metabasalt and metabasaltic flows (Fig. 7). All samples have high Cr content >60 ppm, which is in accordance with oceanic basalts (cf. Morales-Gámez *et al*., 2009; Fig. 7).

Bustamante and Aramberri trace-element compositions are similar but differ from Novillo and Peregrina compositions. In the Bustamante and Aramberri Uplift rocks, the large incompatible elements Sr (0.6–4 ppm), K (0.05–10 ppm), Rb (11–21 ppm) and Ba (0.8–41 ppm; Fig. 8a and b), have scattering mid-ocean-ridge-basalt (MORB) normalized values (Fig. 8). This indicates mobility of these elements during metamorphism (cf. Humphris and Thompson, 1978).

An alkaline affinity is documented for these rocks suites by Zr/Ti of 0.01 and Nb/Y ratios of 0.80–1.4 (Fig. 9a). Ti/V ratios of 45–55 both for Bustamante and Aramberri rocks (Fig. 9b) indicate an ocean-island basalt composition. This is in accordance with Zr/Y of 6–8 and Zr/Nb of 4–9, which point to a derivation from an enriched mantle source or possible contribution of a mantle plume (cf. Sun and McDonough, 1989). Values of ΔNb# ($1.74 + \log(Nb/Y) - 1.92 \times \log(Zr/Y)$) of 0.0 to +0.4 for the metabasalt and metapillow lava match with the ΔNb# of enriched MORB. Hf/Th, both incompatible elements, ranges between 1.5 and 3.1, and the Th/Nb ratio is between 0.08 and 0.1 (cf. Wood, 1980; Saunders *et al*., 1988). These values are typical for ocean-island basalt (Fig. 9c). The rocks are enriched in light REE with LaN/YbN of 4.8–8.8 and LaN/SmN of 1.6–2.6 (*N* = normalized values after Sun and McDonough, 1989; Fig. 10a and b). Europium anomalies are not present (Eu/Eu* = 0.9–1.1).

Incompatible trace element concentrations in metabasaltic rocks of the Peregrina and Novillo Canyons are similar to MORB and differ from the higher trace element concentrations of the Bustamante and Aramberri Uplift rocks. Likewise, the Bustamante and Aramberri samples, K, Rb and Ba, have highly scattered values (K = 0.2–2 ppm, Rb = 0.4–4.5 ppm and Ba = 3 ppm; Fig. 8c and d) in the Peregrina and Novillo samples, which mean that the concentrations of these elements were also affected by metamorphism.

A subalkaline affinity is given by Zr/Ti of 0.01 and Nb/Y of <0.4 (Fig. 9a) for the Peregrina and Novillo Canyons rocks. The Ti/V ratio of 29–44 indicates an ocean floor basalt composition (cf. Vasconcelos *et al*., 2001; Fig. 9b). A low Zr/Y ratio of 0.9–3 and a clearly higher Zr/Nb ratio of 14–53 can be referred to a depleted mantle source in the Peregrina and Novillo Canyons rocks. All rocks have similar Hf/Th ratios of 4.4–14 and Th/Nb ratios of 0.08–0.15, which are typical values for MORB (Fig. 9c). The REE patterns of the Peregrina and Novillo Canyon rocks are flat with LaN/YbN ratio of 0.74–1.7, and they are partly depleted in light REE with LaN/SmN ratios of 0.60–1.4, which resemble the average composition of normal MORB (N-MORB) mantle derived melts (Fig. 10c and d). The only exception is the metabasaltic flow from the Peregrina Canyon (sample CPS8), which is slightly enriched in light REE with LaN/YbN of 3.2, LaN/SmN of 1.5 and depleted in heavy REE with SmN/YbN of 2.08. This indicates a more enriched and deeper source, almost like those of the Aramberri and Bustamante rocks. The Eu/Eu* values for the Peregrina and Novillo Canyon rocks are 0.9–1.1. All the investigated

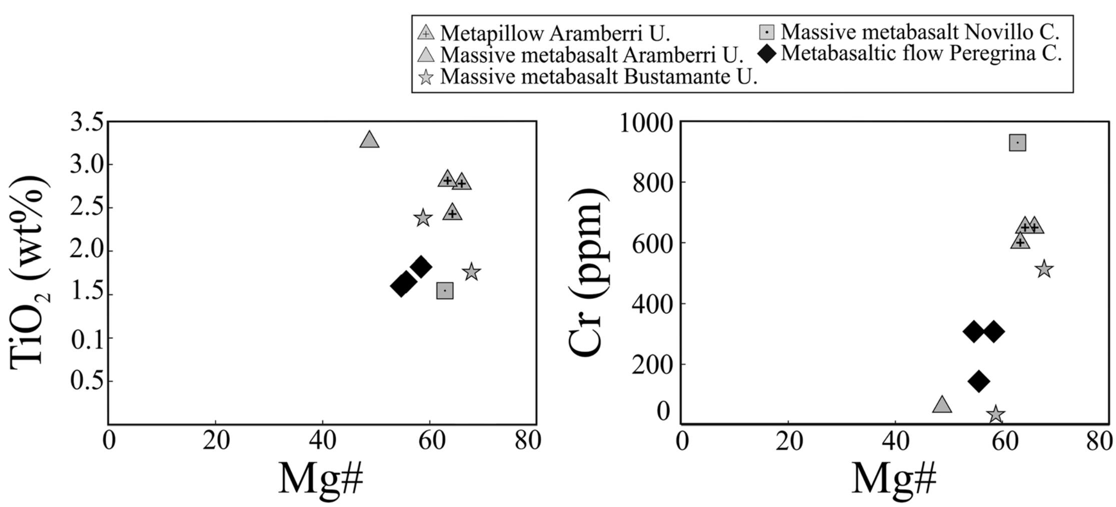

Figure 7. Mg# versus TiO_2 and Cr for the metavolcanic rocks.

DOI: 10.1002/gj

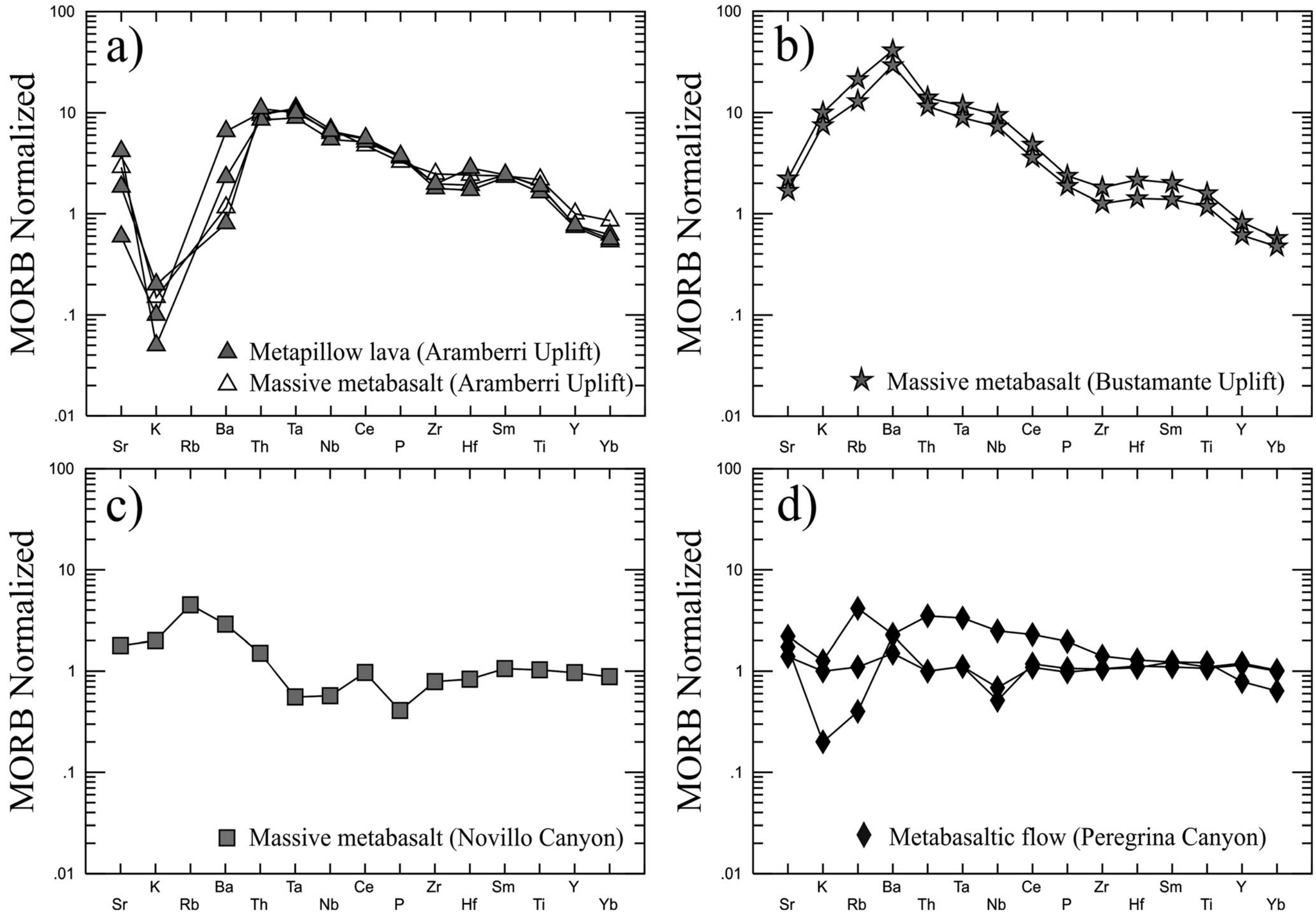

Figure 8. Multi-elemental diagrams. MORB, mid-ocean ridge basalt. Normalizing values after Pearce (1980).

rocks have low La/Ta of <19, La/Nb <2 and Th/Nb <0.11 indicating no crustal contamination.

Major and trace elements have been widely used in conventional discrimination diagrams to identify different tectonic settings (e.g. Pearce and Cann, 1973; Wood, 1980; Shervais, 1982; Meschede, 1986; Cabanis and Lecolle, 1989). However, their application has been criticized (Verma, 2010) because (a) the discriminations only use bi- or trivariate data drawn from 'closed' arrays, (b) the diagrams were generally constructed using a limited geochemical database, (c) they do not incorporate statistical treatment for compositional data (Aitchison, 1986) and (d) such diagrams only discriminate broadly grouped settings (cf. Velasco-Tapia and Verma, 2013). Contrastingly, the discrimination diagrams of Agrawal *et al*. (2008) and Verma and Agrawal (2011) are based on equations that use natural logarithm transformed ratios of TiO_2ADJ and the immobile elements La, Sm, Yb and Nb, using Th as the common denominator.

The rocks from the Aramberri and Bustamante Uplifts have an ocean-island basalt composition according to the discriminative functions of Agrawal *et al*. (2008) and Verma and Agrawal (2011; Fig. 11; Appendix 10, see Supporting Information), as well as with traditional discriminants. Similarly, the composition of the metabasalt from the Peregrina and Novillo Canyons, indicated to be N-MORB by its trace-element ratios, is in agreement with a MORB origin (Fig. 11).

6. $^{40}Ar/^{39}Ar$ GEOCHRONOLOGY

The Ar–Ar results for the three aliquots of muscovite from CPS11 are quite similar (Appendix 11, see Supporting Information). The plateau ages are 299.6 ± 1.7 Ma (MSWD = 1.67), 302.3 ± 1.9 Ma (MSWD = 0.51) and 298.7 ± 1.1 Ma (MSWD = 1.11; Fig. 12). The plateaus have a reliable total ^{39}Ar release of 85% for steps 3 to 9 in aliquot 1 (Fig. 12a). Aliquot 2 has 59% of ^{39}Ar release for steps 12 to 14 (Fig. 12b) and aliquot 3 released 75% of the ^{39}Ar during steps 26 to 30 (Fig. 12c). The average of the three ages is 300 ± 4 Ma (MSWD = 5.4), which we consider as the age of metamorphism.

DOI: 10.1002/gj

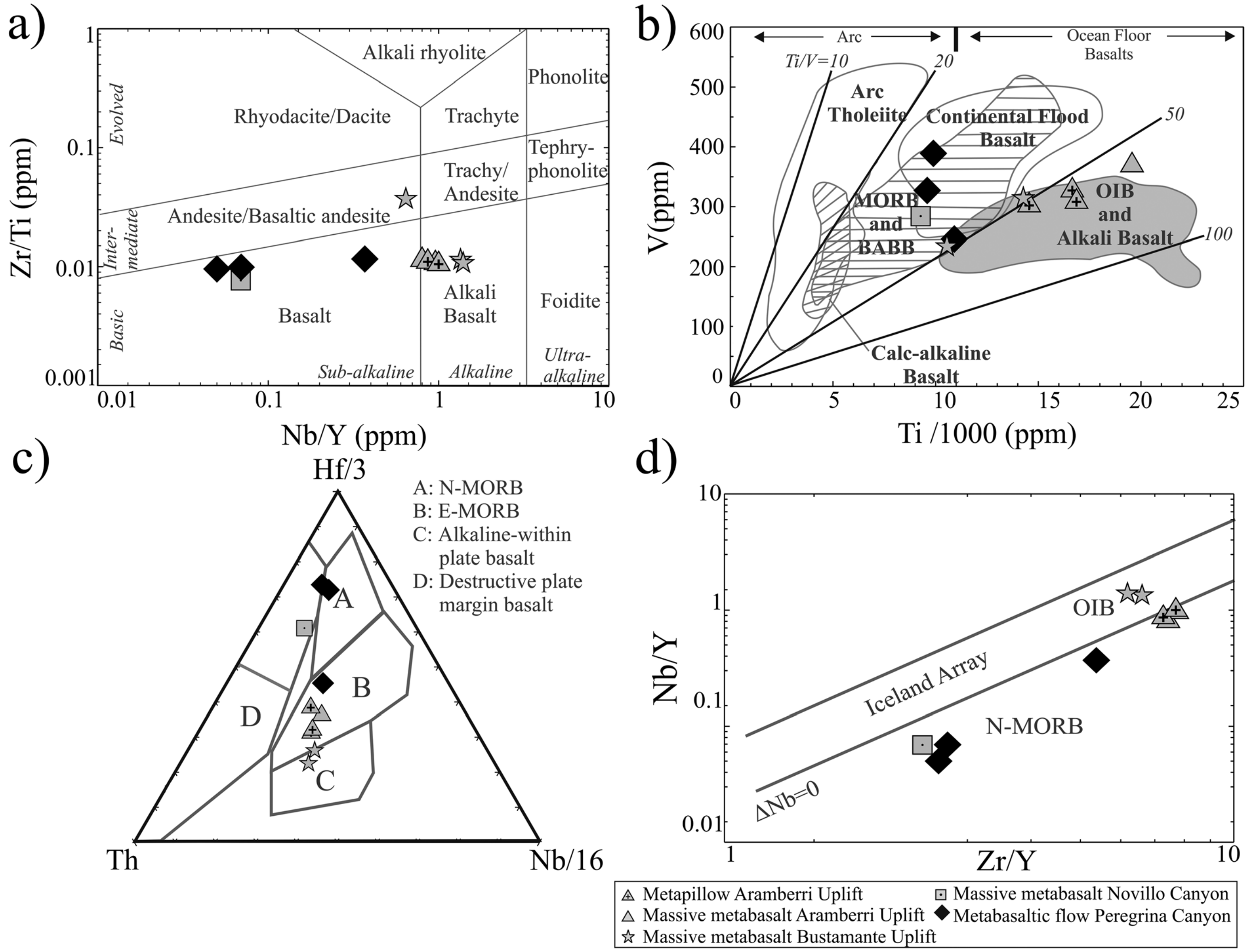

Figure 9. (**a**) Zr/Ti versus Nb/Y for metavolcanic rocks after Winchester and Floyd (1977), (**b**) Ti-V discrimination diagram for basalt after Shervais (1982). The straight lines represent different Ti/V ratios, (**c**) tectonomagmatic discrimination plot after Wood (1980) and (**d**) Nb/Y and Zr/Y variation for Icelandic basalt and normal MORB (after Fitton *et al*., 1997, 2003). BABB, back-arc basin basalt; MORB, mid-ocean ridge basalt; N-MORB, normal MORB; E-MORB, enriched MORB; OIB, ocean-island basalt.

7. INTERPRETATION

7.1. Alterations

According to low indices of alteration, the mafic rocks have undergone incipient chemical alteration during seafloor weathering and regional metamorphism (cf. Ishikawa *et al*., 1976; Nesbitt and Young, 1982; Gifkins *et al*., 2005).

The abundances of most major and some trace elements, especially alkalis, are susceptible to alteration by metamorphism (e.g. Grapes, 1976). The elevated loss on ignition values and variable abundances of Ba, K, Rb and Sr (Fig. 8) in the studied samples are attributed to seafloor and metamorphic processes. This is supported by the presence of quartz, calcite, chlorite and phengitic aluminoceladonite-filled amygdales, which is petrographic evidence for local mobility of major and some trace elements. The elevated Na_2O content indicates alteration through ocean-floor processes and low-grade metamorphism reflected by crystallization of albite. Mg-, Ca-, Al- and K-mobility are represented by the possible replacement of olivine by chlorite and plagioclase phenocrysts by albite, pumpellyite and/or epidote.

In the analysed rocks, most major elements were mobile. However, the concentration of high field-strength elements, REE and the transition elements V, Cr, Ni and Sc are thought to be unaffected by seafloor alteration processes and low-grade metamorphism (Winchester and Floyd, 1976; Wood, 1980; Bienvenu *et al*., 1990). Therefore, we use only immobile element ratios to discriminate the tectonic setting and provide information about the primary source for the subgreenschist to greenschist facies metabasalt (e.g. Pearce and Cann, 1973).

DOI: 10.1002/gj

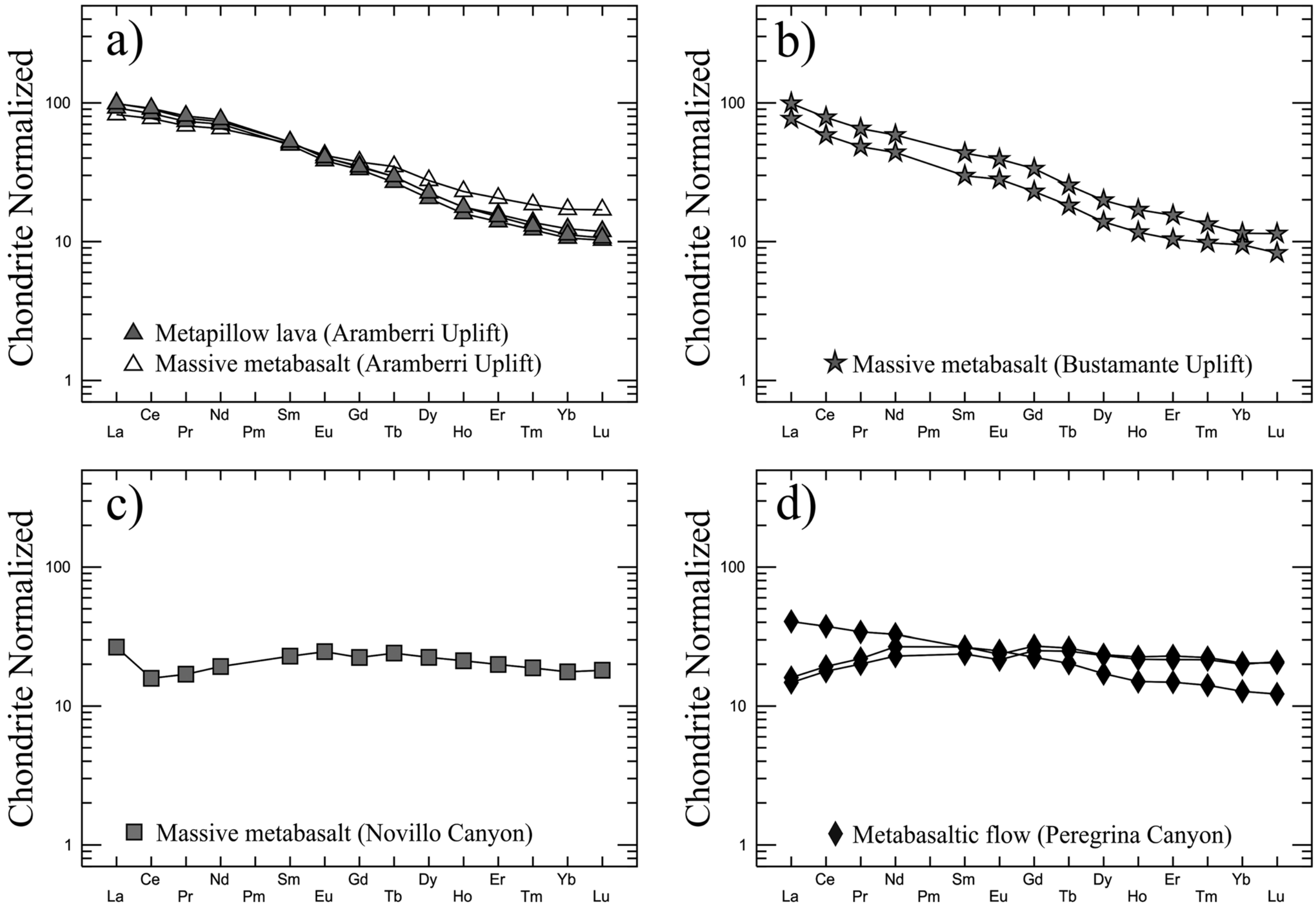

Figure 10. Rare earth element abundances in the metavolcanic rocks. Normalizing values after Sun and McDonough (1989).

7.2. Tectonomagmatic setting determination

The compositional differences between magma types from the different areas can be essentially related to different source characteristics that are associated with formation in distinct tectonomagmatic settings (e.g. Pearce, 1982; Shervais, 1982). We assume a mid-ocean ridge origin for the metavolcanic rocks from the Peregrina and Novillo Canyon based on their flat REE patterns and the discrimination functions of Agrawal *et al*. (2008) and Verma and Agrawal (2011). The composition of the massive metabasalt and metabasaltic flows is comparable to subalkaline, tholeiitic N-MORB from a depleted magma source as evidenced by the low Zr/Ti, Nb/Y and Zr/Y ratios (Fig. 9a and d) as well as the negative ΔNb# values and high Hf/Th and Ti/V ratios (cf. Winchester and Floyd, 1977; Wood, 1980; Shervais, 1982; Meschede, 1986; Fitton *et al*., 1997, 2003).

In contrast to the rocks from the Novillo and Peregrina Canyon, the high TiO_2 wt%, Nb/Y and Ti/V ratios and low Hf/Th and Zr/Ti ratios indicate that the alkaline basalt from the Aramberri and Bustamante Uplifts may be directly derived from a more enriched, deeper asthenospheric mantle source comparable to that of OIB. This is supported by the relict clinopyroxene phenocrysts in the Aramberri and Bustamante Uplift basalt (cf. Beccaluva *et al*., 1989; Fig. 5). Their high Zr/Y, low Zr/Nb and positive ΔNb# values also are in accordance with within-plate basalt, displaying OIB signatures (cf. Sun and McDonough, 1989). The fractionated REE patterns with low contents of HREE may also be indicators in regard of their OIB-like generation. This evidence is further supported by the discrimination diagrams of Agrawal *et al*. (2008) and Verma and Agrawal (2011), showing OIB-like composition for the metabasalt (Fig. 11). Hence, we can assume that the basalts may represent seamount material related with a plume-like source.

Only the light REE-enriched metabasaltic flow from the Peregrina Canyon (sample CPS08) corresponds to enriched MORB and hence to a different extrusion environment. Even so, its REE pattern is similar to that of the OIB-like basalt from the Aramberri and Bustamante Uplifts (Fig. 10). The high Zr/Y and Nb/Y ratios indicate

DOI: 10.1002/gj

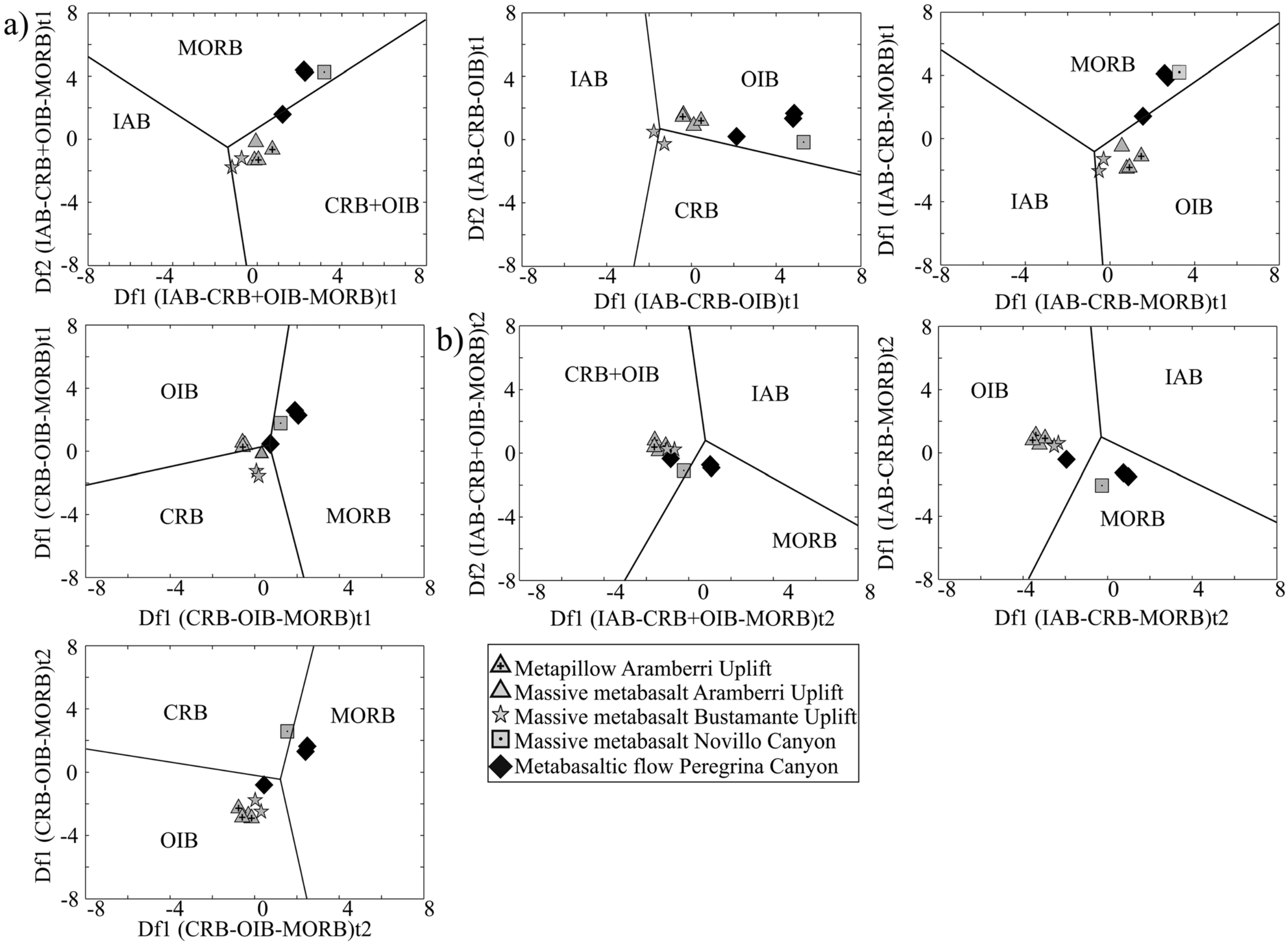

Figure 11. (**a**) Set of tectonomagmatic discrimination diagrams based on natural logarithm transformation of trace-element ratios discriminant function DF1–DF2 (according to Agrawal *et al*. 2008) and (**b**) natural logarithm-transformed ratios of (TiO_2), V, Y, Nb and Zr (according to Verma and Agrawal, 2011). All data are plotted in the diagrams; only applicable discriminant functions are shown. CRB, continental rift basalt; IAB, island arc basalt; MORB, mid-ocean ridge basalt; OIB, ocean-island basalt.

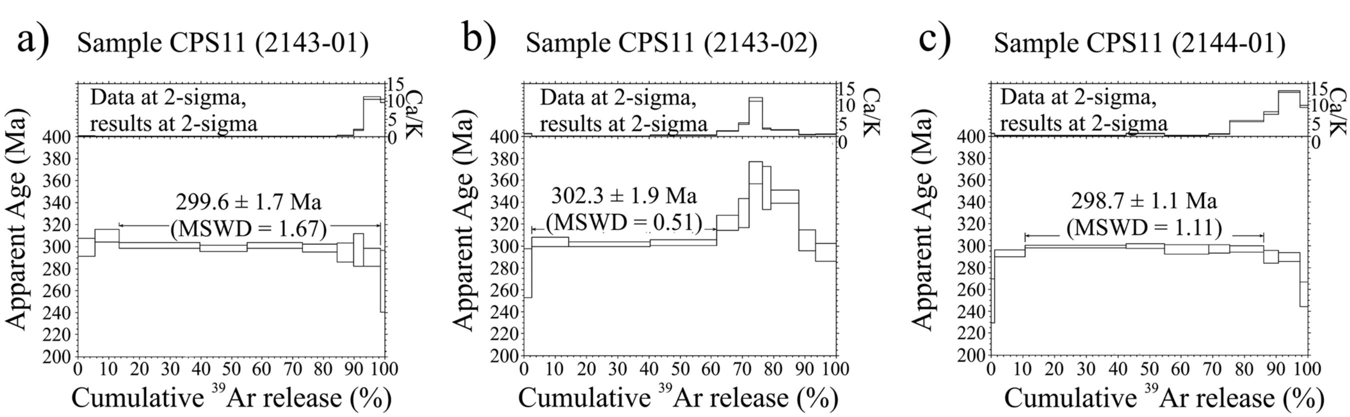

Figure 12. Muscovite $^{40}Ar/^{39}Ar$ plateau age diagrams for the three aliquots of metabasaltic lava flow sample CPS11.

DOI: 10.1002/gj

a source formed by partial melting of a mantle that is enriched, for example, in Nb relative to N-MORB. This enrichment may have occurred by addition of a small fraction of plume-type mantle to a MORB-like mantle (cf. Fitton, 2007). The fact that the metabasaltic flow from the Peregrina Canyon is showing an E-MORB signature supports a possible interaction between depleted MORB mantle and OIB-type mantle components. This could indicate that all sampled basalts originated more or less coeval and close-by in a rift and an off-axis situation in the ocean basin.

7.3. *Metamorphic conditions*

In all studied samples, metamorphic recrystallization is characterized by the replacement of phenocrysts and interstitial areas by a varied suite of low-grade metamorphic minerals such as chlorite, albite and pumpellyite. The albitization of feldspar released Ca and Al ions and supported the formation of calcite, mafic phyllosilicates and calc-silicates (prehnite, pumpellyite and epidote).

Petrographic characteristics suggest that the volcanic rocks metamorphosed under low-pressure conditions. According to Winkler (1979), the absence of lawsonite and/or glaucophane-bearing assemblages indicates pressures below 3 kbar at the calculated temperatures of up to 350 °C. This is consistent with Si of 3.4 apfu in the phengitic mica, which corresponds to 2.5–4 kbar, i.e. approximately greenschist facies (cf. Velde, 1965; Massonne and Schreyer, 1987). Furthermore, the presence of pumpellyite, actinolite and epidote and the absence of prehnite + actinolite in the MORB-type rocks suggest recrystallization at pressures near the pumpellyite ± actinolite ± greenschist facies, i.e. at about 2.5 kbar (cf. Velde, 1965; Massonne and Schreyer, 1987).

In the metavolcanic rocks of the Aramberri and Bustamante Uplifts, the presence of quartz, calcite, chlorite and filling of amygdales and veins is consistent with alteration produced by hydrothermal fluids percolating under static conditions during ocean-floor spreading. The assemblages of chlorite + epidote + prehnite + actinolite + pumpellyite in different combinations are in accordance with prehnite–pumpellyite and pumpellyite–actinolite facies metamorphism. Furthermore, the high Si/Al ratio, low Na_2O and TiO_2, contents and the high cationic ratios of the phengitic aluminoceladonite are in agreement with subgreenschist facies, as well as with the chlorite temperatures below 300 °C.

In contrast to the subgreenschist facies in the Aramberri and Bustamante Uplift areas, the chlorite temperatures above 300 °C and the generally obliterated primary igneous textures for the N-MORB rocks in the Peregrina and Novillo Canyons indicate greenschist facies. This is supported by the high cationic ratios of the phengite in the Peregrina Canyon (cf. Wise and Eugster, 1974; Kawachi, 1975; Coombs *et al*., 1976; Guidotti and Sassi, 1998). Furthermore, the diagnostic assemblage actinolite + epidote + chlorite + albite and quartz in one investigated metabasaltic flow from the Peregrina Canyon indicates the onset of greenschist facies conditions (cf. Bucher and Grapes, 2011). The timing of greenschist facies conditions is determined by the Ar–Ar age of 300 ± 4 Ma from the Peregrina Canyon, which is similar to previous Ar–Ar age data of the metasedimentary part of the Granjeno Schist in the Novillo Canyon (e.g. Dowe *et al*., 2005). The Ar–Ar age indicates the metamorphic phase rather than a cooling age because the chlorite temperatures are above the blocking temperature for the K–Ar system in mica. These inferred metamorphic conditions disagree from previous studies that are largely based on petrographic analysis. In former studies, solely greenschist facies metamorphism was realized for the Granjeno Schist (Carrillo-Bravo, 1961; De Cserna and Ortega-Gutiérrez, 1978; Ramírez-Ramírez, 1974, 1992; Dowe *et al*., 2005).

7.4. *Tectonic model*

The metavolcanic rocks of the present study record the evolution from seafloor volcanism at an ocean ridge, over the extrusion of alkaline intraplate volcanic rocks onto the oceanic crust, up to their low-grade metamorphism in a subduction zone. As there are no indications for geochemical involvement of either continental crust or subduction magmatism in the volcanic protoliths of the Granjeno Schist, we suggest that the magmatic evolution was completely within an oceanic plate. The schematic model that we propose (Fig. 13a) postulates the extrusion of N-MORB along a mid-ocean ridge (Novillo and Peregrina Canyons) with contribution of an alkaline intraplate-type magma source [Aramberri and Bustamante Uplifts (Fig. 13a)].

Depositional contacts of clastic (continental) metasedimentary rocks with the mafic metavolcanic rocks throughout the Granjeno Schist indicate that the sedimentation was contemporaneous with the volcanism, probably as a result of progradation of continental sediment over the ocean floor. The age of the basaltic rocks is unknown, but maximum depositional ages of the coeval metasedimentary rocks are late Cambrian to Devonian (Barboza-Gudiño *et al*., 2011; Torres-Sánchez *et al*., 2013), possibly indicating a composite unit with a long sedimentation and volcanism history. Grenvillian (1250–920 Ma) and Pan-African (730–530 Ma) zircon crystallization ages suggest that the Novillo Gneiss of the Oaxaquia microcontinent and the Gondwana continent may have been the main sediment sources (Barboza-Gudiño *et al*., 2011; Torres-Sánchez *et al*., 2013). Thus,

DOI: 10.1002/gj

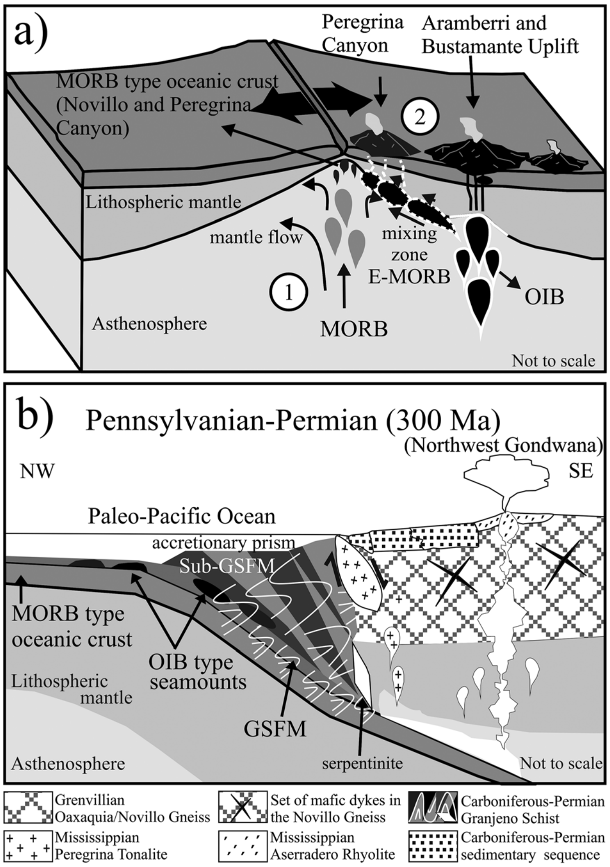

Figure 13. (**a**) Sketch model showing the supposed tectonic setting of the metavolcanic rocks. 1: extrusion of N-MORB along a mid-ocean ridge, 2: formation of enriched mid-ocean-ridge basalt and ocean-island basalt. The ocean-island basalt-type rocks formed from an enriched, deep mantle source, whereas enriched mid-ocean-ridge basalt formed due to mixing of the OIB-type and MORB magmas, (**b**) low-grade metamorphism and juxtaposition of sedimentary and oceanic rocks in a subduction zone at NW Gondwana during Pennsylvanian–Permian time. N-MORB, normal mid-ocean ridge basalt; E-MORB, enriched MORB basalts; GSFM, greenschist facies metamorphism; OIB, ocean-island basalt.

the Granjeno Schist can be related to the Rheic Ocean. Today, the Novillo Gneiss is exposed in the Peregrina and Novillo Canyons with tectonic contacts to the younger rocks.

Assuming that the youngest maximum depositional ages are similar to the youngest depositional part of the Granjeno Schist, N-MORB igneous activity and sedimentation in the Novillo and Peregrina Canyon area lasted at least from Silurian to Devonian time. The extrusion of N-MORB from asthenospheric magma can be related with rifting and drifting of the Rheic Ocean during that time.

The OIB in the Aramberri and Bustamante Uplifts as well as the E-MORB in the Peregrina Canyon indicate low degree melting of an enriched, deep mantle source, which often is ascribed to disperse blobs of enriched material in the depleted upper mantle or to the involvement of a mantle plume (cf. Fitton *et al*., 1997, 2003). This relatively contemporaneous activity of an enriched source near the spreading axis also enriched the MORB-type magmatism. Thus, the OIB may have derived from the deep mantle melting source itself and the E-MORB magma from shallower levels, where melts of OIB and N-MORB inevitably mixed. The OIB and the metasedimentary rocks of the Aramberri Uplift are in fault contact today due to a younger tectonic event.

Regional studies about the southern and northeastern Mexico indicate that the closure of the Rheic Ocean did not result in a continent–continent collision but moved Gondwana into contact with the Paleo-Pacific Ocean (e.g. Dickinson and Lawton, 2001; Nance *et al*., 2007; Keppie *et al*., 2008). As a result, dextral transpression took place and a Pennsylvanian–Permian magmatic arc was established (cf. Nance *et al*., 2007, 2012; Keppie *et al*., 2010, 2012; Barboza-Gudiño *et al*., 2011). The metamorphic age of 300 ± 4 Ma indicates that the metamorphic overprint of the volcano-sedimentary rocks of the present study may have taken place in an accretionary prism during Pennsylvanian to Permian time (cf. Barboza-Gudiño *et al*., 2011). The Aramberri and Bustamante OIB rocks would have been integrated at shallower depth into the accretionary prism under subgreenschist facies conditions (Fig. 13b). The higher-grade metamorphism of the Novillo and Peregrina Canyons rocks took place at larger depths within the subduction channel (Fig. 13b).

Former interpretations suggest that metamorphism of the Granjeno Schist was caused by the collision of Laurentia with Gondwana during Carboniferous time (Garrison *et al*., 1980; Ramírez–Ramírez, 1992; Dowe *et al*., 2005; Nance *et al*., 2007). Garrison *et al*. (1980), Ortega-Gutiérrez (1981) and Ramírez–Ramírez (1992) assumed that the volcanic rocks formed along an active margin in the Iapetus Ocean and underwent greenschist facies metamorphism during the Pangaea-forming collision of Gondwana with Laurentia. The estimated low metamorphic pressures for the Granjeno Schist are not typical for a continent–continent collision. Instead, obduction and accretion in an evolving active margin is more plausible. It is in accordance with the metamorphic age of the Granjeno Schist as well as with the presence of plagiogranite with syn-collisional and volcanic-arc characteristics, which intruded the Novillo Gneiss at *ca*. 350 Ma (Dowe *et al*., 2005; De León Barragán, 2012). The time of the enriched volcanism is unclear. It could be related to Silurian plume magmatism at the Oaxaquia margin in southern Mexico before collisional time as suggested by Keppie *et al*. (2007), or the OIB source components were present as blobs of enriched material carried in the upper mantle convective flow and responsible for OIB seamounts and E-MORB during the Silurian to Devonian time. Another possibility is the association with a Mississippian–Permian plume located in the Paleo-Pacific Ocean as described by Tatsumi *et al.* (2000).

8. CONCLUSIONS

We suggest a mid-ocean ridge that formed N-MORB ocean crust during the rifting of the Rheic Ocean. Rifting of the Rheic Ocean was accompanied by transcurrent faulting that supported the migration of southwest Gondwana during the closure of the Rheic Ocean and Pangaea formation. During the propagation of the ocean floor, the mid-ocean ridge volcanism was accompanied by alkalic intraplate volcanism to form both the E-MORB and the ocean-island basalt of the Granjeno Schist. Our model implies a more complex palaeotectonic framework than earlier assumed for the evolution of the Granjeno Schist. Contradictory to previous assumptions, the model implies that northeastern Mexico was not part of a collisional event between Laurentia and Gondwana. Instead we emphasize that a circum-Pangaea non-collisional subduction zone, which caused prograde metamorphism in northeastern Mexico, was active during Pennsylvanian to Permian time. The metavolcanic rocks of the Granjeno Schist then became part of Pangaea by accretion. The processes that formed the Granjeno Schist represent a part of the closure of the Rheic Ocean and convergence tectonics along the Paleo-Pacific margin after the Laurentia and Gondwana collision.

ACKNOWLEDGEMENTS

We would like to acknowledge PaicyT and Facultad de Ciencias de la Tierra, Universidad Autónoma de Nuevo León (UANL), Mexico, for supporting the field work and Dr Uwe Jenchen who supported the whole-rock chemical analysis. Microprobe analyses were funded by the Institute of Geosciences, Friedrich-Schiller University Jena (FSU), Germany and the Best Thesis Award 2010 granted by UANL. The geochronological analyses were funded by the SEP-CONACYT 000169231 project headed by Dr José Rafael Barboza Gudiño, Universidad Autónoma de San Luis Potosí, Mexico. S. T. S. acknowledges ConacyT for a research stay at the Institute of Geosciences, FSU, during 2012, financed by the Scholarship 'Becas Mixtas 2012–2013 Movilidad en el extranjero' (scholarship number 239341) and to DAAD for the 'Research Grant for Doctoral Candidates and Young Academics and Scientists 2013–2015' (scholarship number 57076385). We also thank Dr Calixto Ramírez-Ramírez and Dr Leon E. Long who facilitated search for old literature about the study area, Dr Surendra Pal Verma Jaiswal, Dr Sanjeet Kumal Verma and MSc Maria Abdelaly Rivera Gómez that helped with the use of IgRocks and TecD and Dr Fernando Velasco-Tapia and Dr Daniel Beyer for the discussions during the writing of this paper. We also thank to Dr. Leon E. Long and the anonymous reviewer for their comments that improved the paper.

REFERENCES

Agrawal, S., Guevara, M., Verma, S.P. 2008. Tectonic discrimination of basic and ultrabasic volcanic rocks through log-transformed ratios of immobile trace elements. *International Geology Review* **50**(12), 1057–1079.

Aitchison, J. 1986. *The Statistical Analysis of Compositional Data*. Chapman and Hall: London; 416.

Armstrong-Altrin, J.S. 2015. Evaluation of two multidimensional discrimination diagrams from beach and deep-sea sediments from the Gulf of Mexico and their application to Precambrian clastic sedimentary rock. *International Geology Review* **57**(11–12), 1446–1461.

Barboza-Gudiño, J.R., Gómez-Anguiano, M., Zavala-Monsiváis, A. 2008. The Early Mesozoic volcanic arc of western North America in northeastern Mexico. *Journal of South American Earth Sciences* **25**(1), 49–63.

Barboza-Gudiño, J.R., Ramírez-Fernández, J.A., Torres-Sánchez, S.A., Valencia, V.A. 2011. Geocronología de circones detríticos de diferentes localidades del Esquisto Granjeno en el noreste de México. *Boletín de la Sociedad Geológica Mexicana* **63**(2), 201–216.

Beccaluva, L., Macciotta, G., Piccardo, G.B., Zeda, O. 1989. Clinopyroxene composition of ophiolite basalts as petrogenetic indicator. *Chemical Geology* **77**(3), 165–182.

Bienvenu, P., Bougault, H., Joron, J.L., Treuil, M., Dmitriev, L. 1990. MORB alteration: rare-earth element/non-rare-earth hygromagmaphile element fractionation. *Chemical Geology* **82**, 1–14.

Blakey, R.C. 2007. Carboniferous–Permian paleogeography of the assembly of Pangea. In: *Fifteenth International Congress on Carboniferous and Permian Stratigraphy*, Wong, T.E. (ed.). Royal Netherlands Academy of Arts and Sciences: Amsterdam; 443–465.

Bucher, K., Grapes, R. 2011. *Petrogenesis of Metamorphic Rocks*. Springer: Berlin Heidelberg; 21–56.

Cabanis, B., Lecolle, M. 1989. Le diagramme La/10-Y/ 15-Nb/8: un outil pour la discrimination des series volcaniques et la mise en evidence des processus de melange et/ou de contamination crustale. *Comptes Rendus de l'Académie des Sciences* **11**(309), 2023–2029.

Cameron, K.L., Lopez, R., Ortega-Gutiérrez, F., Solari, L., Keppie, J.D., Schulze, C. 2004. U-Pb geochronology and Pb isotope compositions of leached feldspars: constraints on the origin and evolution of Grenvillian rocks from eastern and southern Mexico. In: *Proterozoic Tectonic Evolution of the Grenville Orogen in North America*, Tollo, R.P., Corriveau, L., McLelland, J.B., Bartholemew, G. (eds.). Geological Society of America Memoir: Boulder **197**; 755–769.

Campa, M.F., Coney, P.J. 1983. Tectono-stratigraphic terranes and mineral resource distributions in Mexico. *Canadian Journal of Earth Sciences* **20**(6), 1040–1051.

Carrillo-Bravo, J. 1961. Geología del Anticlinorio Huizachal-Peregrina al NW de Ciudad Victoria, Tamaulipas. *Boletín de la Asociación Mexicana de Geólogos Petroleros* **13**(1-2), 1–98.

Castillo-Rodríguez, H. 1988. *Zur Geologie des kristallinen Grundgebirges der Sierra Madre Oriental – insbesondere des Granjeno-Schiefer-Komplexes im Südteil des Huizachal–Peregrina–Antiklinoriums (Raum Ciudad Victoria, Tamaulipas, Mexiko)*. MSc. Thesis, University of Münster, 138.

Cathelineau, M. 1988. Cation site occupancy in chlorites and illites as a function of temperature. *Clay Minerals* **23**, 471–485.

Cawood, P. A., Kröner, A., Collins, W. J., Kusky, T. M., Mooney, W. D., Windley, B. F. 2009. *Accretionary orogens through Earth history*. Geological Society of London, Special Publications **318**, 1–36.

Coombs, D.S., Nakamura, Y., Vuagnat, M. 1976. Pumpellyite-actinolite facies schists of the Taveyanne Formation near Loèche, Valais, Switzerland. *Journal of Petrology* **17**, 440–447.

DOI: 10.1002/gj

Cossío Torres, T. 1988. *Zur Geologie der Sierra Madre Oriental - insbensondere des Novillo - -Gneis - Komplexes - im Südteil des Huizachal-Peregrina-Antiklinoriums (Raum Ciudad Victoria, Tamaulipas, Mexiko)*. MSc. Thesis, University of Münster, 99.

De Cserna, Z., **Ortega-Gutiérrez, F. 1977**. Alóctono del Paleozoico inferior en la región de Ciudad Victoria, estado de Tamaulipas. *Boletín del Instituto de Geología de la Universidad Nacional Autónoma de México* **1**, 33–43.

De Cserna, Z., **Ortega-Gutiérrez, F. 1978**. Reinterpretation of isotopic age data from the Granjeno Schist, Ciudad Victoria, Tamaulipas. *Revista Mexicana de Geociencias de la Universidad Nacional Autónoma de México* **2**, 31–36.

De León Barragán, L. 2012. *Magmatismo ácido en el Basamento de la Sierra Madre Oriental, Anticlinorio Huizachal Peregrina, Tamaulipas, México*. B.S. Thesis, Universidad Autónoma de Nuevo León, 153.

Denison, R.E., **Burke, W.H., Jr.**, **Hetherington, E.A.**, **Otto, J.B. 1971**. Basement rock framework of parts of Texas, southern New Mexico and northern Mexico. In: *The Geologic Framework of the Chihuahua Tectonic Belt: Midland, Texas*, Seewald, K. Sundeen, D. (eds.). West Texas Geological Society Publications: Midland; 3–14.

Dickin, A.P. 2005. *Radiogenic Isotope Geology*. Cambridge University Press: UK; 492.

Dickinson, W.R., **Lawton, T.F. 2001**. Carboniferous to Cretaceous assembly and fragmentation of Mexico. *Geological Society of America Bulletin* **113**(9), 1142–1160.

Dowe, D.S., **Nance, R.D.**, **Keppie, J.D.**, **Cameron, K.L.**, **Ortega-Rivera, A.**, **Ortega-Gutiérrez, F.**, **Lee, J.W.K. 2005**. Deformational history of the Granjeno Schist, Ciudad Victoria, Mexico: constraints on the closure of the Rheic Ocean? *International Geology Review* **47**(9), 920–937.

Ehricke, C. 1998. *Mafische und ultramafische Gesteine des Novillo-Canyons, Sierra Madre Oriental, Mexiko*. Diploma Thesis, Universität Freiburg, Institut für Mineralogie, Petrologie und Geochemie der Albert- Ludwigs, **93**.

Fitton, J.G., **Saunders, A.D.**, **Norry, M.J.**, **Hardarson, B.S.**, **Taylor, R. N. 1997**. Thermal and chemical structure of the Iceland plume. *Earth and Planetary Science Letters* **153**(3), 197–208.

Fitton, J.G., **Saunders, A.D.**, **Kempton, P.D.**, **Hardarson, B.S. 2003**. Does depleted mantle form an intrinsic part of the Iceland plume? *Geochemistry, Geophysics, Geosystems* **4**(3), 1032.

Fitton, J.G. 2007. The OIB paradox. In: *Plates, Plumes, and Planetary Processes*, Foulger, G.R. and Jurdy, D.M. (eds.). Geological Society of America, Special Paper **430**: Boulder, Colorado; **430**, 387–415.

Fries, C., **Schmitter, E.**, **Damon, P.E.**, **Livingston, D.E.**, **Erickson, R. 1962**. Edad de las rocas metamórficas de los cañones de la Peregrina y de Caballeros parte centro-occidental de Tamaulipas. *Boletín del Instituto de Geología* **64**, 55–69.

Fries, C., **Rincón-Orta, C. 1965**. Nuevas aportaciones geocronológicas y técnicas empleadas en el laboratorio de geocronología: Universidad Nacional Autónoma de México. *Boletín del Instituto de Geología* **73**, 57–134.

Garrison, J.R., Jr., **Ramírez-Ramírez, C.**, **Long, L.E. 1980**. Rb/Sr isotopic study of the ages and provenance of Precambrian granulite and Paleozoic greenschist near Ciudad Victoria, Mexico. In: *Symposium on the Origin of the Gulf of Mexico and the Early Opening of the Central North Atlantic Ocean*, Pilger, R.H., Jr., (ed.). Louisiana State University: Baton Rouge; 37–49.

Gifkins, C.C., **Herrman, W.**, **Large, R.R. 2005**. *Altered Volcanic Rocks: A Guide to Description and Interpretation*. Centre for Ore Deposit Research University of Tasmania: Tasmania.

Grapes, R.H. 1976. Low grade alteration of basic rocks in Hokkaido, Japan. *Journal of Faculty of Sciences* **4**(L7), 373–385.

Guidotti, C.V., **Sassi, F.P. 1998**. Petrogenetic significance of Na-K white mica mineralogy: recent advances for metamorphic rocks. *European Journal Mineralogist* **10**, 815–854.

Heim, A. 1940. The front ranges of Sierra Madre Oriental, Mexico from Ciudad Victoria to Tamazunchale. *Eclogae Geologicae Helvetiae* **33**(2), 313–352.

Hey, M.H. 1954. A new review of chlorites. *Mineralogical Magazine* **30**, 277–292.

Humphrey, W E. 1954. Stratigraphy of the Cortinas Canyon Section, Sierra de 1os Muertos, Coahuila, Mexico. In: *Twenty First Field Trip Guide Book*, Díaz, T. (ed.). South Texas Geological Society: San Antonio; 89–176.

Humphris, S.E., **Thompson, G. 1978**. Trace element mobility during alteration of oceanic basalts. *Geochimica Cosmochimica Acta* **42**, 127–136.

Imlay, R.W. 1938. Studies of the Mexican geosyncline. *Geological Society of America Bulletin* **49**(11), 1651–1694.

Ishikawa, Y., **Sawaguchi, T.**, **Iwaya, S.**, **Horiuchi, M. 1976**. Delineation of prospecting target for Kuroko deposits based on modes of volcanism of underlying dacite and alteration halos. *Mining Geology* **26**, 105–117.

Jowett, E. C. 1991. *Fitting iron and magnesium into the hydrothermal chlorite geothermometer*. In: *GAC/MAC/SEG, Joint Annual Meeting Program with Abstracts 16*, A-62.

Kawachi, Y. 1975. Pumpellyite-actinolite and contiguous facies metamorphism in part of Upper Wakatipu district, South Island, New Zealand. *Journal of Geology and Geophysics* **18**, 401–41.

Keppie, J.D., **Ortega-Gutiérrez, F. 1995**. Provenance of Mexican terranes: isotopic constraints. *International Geology Review* **37**, 813–824.

Keppie, J.D., **Ortega-Gutiérrez, F. 1999**. Middle American Precambrian basement: a missing piece of the reconstructed 1 Ga orogen. In: *Laurentia-Gondwana Connections Before Pangea*, Ramos, V.A., Keppie, J.D. (eds.). Geological Society of America Special Paper **336**: Boulder Colorado; 199–210.

Keppie, J. D., **Ramos, V.A.R. 1999**. Odyssey of terranes in the Iapetus and Rheic Oceans during the Precambrian. In: *Laurentia Gondwana Connections Before Pangea*, Ramos, V.A., Keppie, J.D. (eds.). Geological Society of America Special Paper **336**: Boulder Colorado; 267–275.

Keppie, J.D. 2004. Terranes of Mexico revisited: a 1.3 billion year odyssey. *International Geology Review* **46**(9), 765–794.

Keppie, J.D., **Dostal, J.**, **Elías-Herrera, M. 2007**. Ordovician–Devonian oceanic basalts in the Cosoltepec Formation, Acatlán Complex, southern México: vestiges of the Rheic Ocean? *Geological Society of America Special Papers* **423**, 477–487.

Keppie, J.D., **Dostal, J.**, **Murphy, J.B.**, **Nance, R.D. 2008**. Synthesis and tectonic interpretation of the westernmost Paleozoic Variscan orogen in southern Mexico: from rifted Rheic margin to active Pacific margin. *Tectonophysics* **461**, 277–290.

Keppie, J.D., **Nance, R.D.**, **Ramos-Arias, M.A.**, **Lee, J.K.W.**, **Dostal, J.**, **Ortega-Rivera, A.**, **Murphy, J.B. 2010**. Late Paleozoic subduction and exhumation of Cambro-Ordovician passive margin and arc rocks in the northern Acatlán Complex, southern Mexico: geochronological constraints. *Tectonophysics* **495**(3), 213–229.

Keppie, J.D., **Nance, R.D.**, **Dostal, J.**, **Lee, J.K.W.**, **Ortega-Rivera, A. 2012**. Constraints on the subduction erosion/extrusion cycle in the Paleozoic Acatlán Complex of southern Mexico: geochemistry and geochronology of the type Piaxtla Suite. *Gondwana Research* **21**(4), 1050–1065.

Ludwig K.R. 2012. *Isoplot 3.75-4.15, a geochronological toolkit for Microsoft Excel. Berkeley Geochronology Center Special Publication* 5.

Massonne, H.J., **Schreyer, R. 1987**. Phengite geobarometry based on the limiting assemblage with k-feldspar, phlogopite and quartz. *Contributions to Mineralogy and Petrology* **96**, 212–224.

Meschede, M. 1986. A method of discriminating between different types of mid-ocean ridge basalts and continental tholeiites with the Nb-Zr-Y diagram. *Chemical Geology* **56**(3), 207–218.

Mickus, K., **Montana, C. 1999**. Crustal structure of northeastern Mexico revealed through the analysis of gravity data. In: *Mesozoic Sedimentary and Tectonic History of North-central Mexico*, C. Bartolini, J. Wilson and T. Lawton, (eds.). Geological Society of America, Special Paper **340**: Boulder Colorado; 357–372.

Mixon, R.B., **Murray, G.E.**, **Diaz, T.G. 1959**. Age and correlation of Huizachal Group (Mesozoic), State of Tamaulipas, Mexico. *Bulletin of American Association Petroleum Geologists* **43**, 757–771.

Morales-Gámez, M., **Keppie, J.D.**, **Dostal, J. 2009**. Carboniferous tholeiitic dikes in the Salada unit, Acatlán Complex, southern Mexico: a record of extension on the western margin of Pangea. *Revista Mexicana de Ciencias Geológicas* **26**(1), 133–142.

DOI: 10.1002/gj

Murillo-Muñetón, G., Anderson, J. L., Tosdal, R. M. 1994. *A new Grenville-age granulite terrane in southern Mexico*. In: *Geological Society of America Program with Abstracts* 26, 2, A-76.

Nance, R. D., Miller, B. V., Keppie, J. D., Murphy, J. B., Dostal, J. 2007. *Vestige of the Rheic Ocean in North America: the Acatlán Complex of southern México. Special Papers Geological Society of America* **423**, p. 437.

Nance, R.D., Linnemann, U. 2008. The Rheic Ocean: origin, evolution, and significance. *GSA Today* **18**(12), 4–12.

Nance, R. D., Keppie, J. D., Miller, B. V., Murphy, J. B., Dostal, J. 2009. *Palaeozoic palaeogeography of Mexico: constraints from detrital zircon age data. Geological Society of London, Special Publications* **327**(1), 239–269.

Nance, R.D., Gutiérrez-Alonso, G., Keppie, J.D., Linnemann, U., Murphy, J.B., Quesada, C., Strachan, R.A., Woodcock, N. 2010. Evolution of the Rheic Ocean. *Gondwana Research* **17**(2–3), 194–222.

Nance, R.D., Gutiérrez-Alonso, G., Keppie, J.D., Linnemann, U., Murphy, J.B., Quesada, C., Woodcock, N.H. 2012. A brief history of the Rheic Ocean. *Geoscience Frontiers* **3**(2), 125–135.

Nesbitt, H.W., Young, G.M. 1982. Early Proterozoic climates and plate motions inferred from major element chemistry of lutites. *Nature* **299**(5885), 715–717.

Orozco-Esquivel, M.T. 1991. *Zur Petrologie des Kristallins im Huizachal – Peregrina - Fenster, Sierra Madre Oriental Mexiko*. Diploma Thesis, University of Karlsruhe, 133.

Ortega-Gutiérrez, F. 1978. El Gneis Novillo y rocas metamórficas asociadas en los Cañones del Novillo y de la Peregrina, área de Ciudad Victoria, Tamaulipas. *Revista del Instituto de Geología, Universidad Nacional Autónoma de México* **2**(1), 19–30.

Ortega-Gutiérrez, F. 1981. Metamorphic belts of southern Mexico and their tectonic significance. *Geofísica Internacional* **20**, 177–202.

Ortega-Gutiérrez, F. 1984. Evidence of Precambrian evaporites in the Oaxacan granulite complex of southern Mexico. *Precambrian Research* **23**(3), 377–393.

Ortega-Gutiérrez, F., Ruíz, J., Centeno-García, E. 1995. Oaxaquia, a Proterozoic microcontinent accreted to North America during the late Paleozoic. *Geology* **23**(12), 1127–1130.

Pantoja-Alor, J., Rincón-Orta, C., Fries, C. Jr., Silver, L.T., Solorio-Munguia, J. 1974. Contribuciones a la geocronología de Chiapas. *Boletín de la Asociación Mexicana de Geólogos Petroleros* **26**, 207–223.

Patchett, P.J., Ruiz, J. 1987. Nd isotopic ages of crust formation and metamorphism in the Precambrian of eastern and southern México. *Contributions to Mineralogy and Petrology* **96**, 523–528.

Pearce, J.A., Cann, J.R. 1973. Tectonic setting of basic volcanic rocks determined using trace element analyses. *Earth and Planetary Science Letters* **19**(2), 290–300.

Pearce, J. A. 1980. *Geochemical evidence for the genesis and eruptive setting of lavas from Tethyan ophiolites*. In: *Proceedings of the International Ophiolite Symposium*. Cyprus 1979; 261–272.

Pearce, J.A. 1982. Trace element characteristics of lavas from destructive plate boundaries. *Andesites* **8**, 525–548.

Ramírez-Ramírez, C. 1974. *Reconocimiento geológico de las zonas metamórficas al poniente de Cd. Victoria, Tamaulipas, México*. B.S Thesis, Universidad Nacional Autónoma de México Facultad de Ingeniería, 78.

Ramírez-Ramírez, C. 1978. *Reinterpretación tectónica del Esquisto Granjeno de Ciudad Victoria, Tamaulipas*. MSc. Thesis. Universidad Nacional Autónoma de México, Facultad de Ingeniería.

Ramírez–Ramírez, C. 1992. *Pre-Mesozoic geology of Huizachal–Peregrina anticlinorium, Ciudad Victoria, Tamaulipas, and adjacent parts of eastern México*. Ph.D Thesis, University of Texas, Austin, 318.

Renne, P.R., Swisher, C.C., Deino, A.L., Karner, D.B., Owens, T.L., DePaolo, D.J. 1998. Intercalibration of standards, absolute ages and uncertainties in ^{40}Ar/^{39}Ar dating. *Chemical Geology* **145**(1), 117–152.

Ruiz, J., Patchett, P.J., Ortega-Gutiérrez, F. 1988. Proterozoic and Phanerozoic basement terranes of Mexico from Nd isotopic studies. *Geological Society of America Bulletin* **100**, 274–281.

Saunders, A.D., Norry, M.J., Tarney, J. 1988. Origin of MORB and chemically-depleted mantle reservoirs: trace element constraints. *Journal of Petrology* **1**, 415–445.

Sedlock, R.L., Ortega-Gutiérrez, F., Speed, R.C. 1993. Tectonostratigraphic terranes and tectonic evolution of Mexico. *Geological Society of America Special Papers* **278**, 1–153.

Shervais, J.W. 1982. Ti-V plots and the petrogenesis of modern and ophiolitic lavas. *Earth and Planetary Science Letters* **59**(1), 101–118.

Silver, L. T., Anderson, T. H., Ortega-Gutiérrez, F. 1994. *The "thousand million year" orogeny in eastern and southern México*. In: *Geological Society of America Program with Abstracts 26*, 7, A-48.

Stampfli, G.M., Borel, G.D. 2002. A plate tectonic model for the Paleozoic and Mesozoic constrained by dynamic plate boundaries and restored synthetic ocean isochrons. *Earth and Planetary Science Letters* **196**, 17–33.

Stewart, J.H., Blodgett, R.B., Boucot, A.J., Carter, J.L., López, R. 1999. Exotic Paleozoic strata of Gondwanan provenance near Ciudad Victoria, Tamaulipas, México. *Geological Society of America Special Papers* **336**, 227–252.

Sun, S.S., McDonough, W. 1989. Chemical and isotopic systematics of oceanic basalts: implications for mantle composition and processes. *Geological Society of London, Special Publications* **42**, 313–345.

Tatsumi, Y., Kani, T., Ishizuka, H., Maruyama, S., Nishimura, Y. 2000. Activation of Pacific mantle plumes during the Carboniferous: evidence from accretionary complexes in southwest Japan. *Geology* **28**(7), 580–582.

Torres-Sánchez, S.A. 2010. *Petrología e Interpretación Geodinámica del Esquisto Granjeno en el Cañón de Caballeros, Anticlinorio Huizachal-Peregrina, NE de México*. B.S. Thesis, Universidad Autónoma de Nuevo León, 186.

Torres-Sánchez, S. A., Augustsson, C., Ramírez Fernández, J.A., Barboza Gudiño, J. R., Jenchen, U., Abratis, M. 2013. *Geochemistry and metamorphism of the Paleozoic metasedimentary basement of the Sierra Madre Oriental, NE Mexico. Possible paths from their depositional environment?*. In: *Geological Society of America Program with Abstracts 45*, 3, A-60.

Vasconcelos, F.M., Verma, S.P., Vargas, B.R.C. 2001. Diagrama Ti-V: una nueva propuesta de discriminación para magmas básicos en cinco ambientes tectónicos. *Revista Mexicana de Ciencias Geológicas* **18**(2), 162–174.

Velasco-Tapia, F., Verma, S.P. 2013. Magmatic processes at the volcanic front of Central Mexican Volcanic Belt: Sierra de Chichinautzin volcanic field (Mexico). *Turkish Journal of Earth Sciences* **22**(1), 32–60.

Velde, B. 1965. Phengite micas: synthesis, stability and natural occurrences. *American Journal of Science* **263**, 886–913.

Verma, S.P. 2010. Statistical evaluation of bivariate, ternary and discriminant function tectonomagmatic discrimination diagrams. *Turkish Journal of Earth Sciences* **19**(2), 185–238.

Verma, S.P., Agrawal, S. 2011. New tectonic discrimination diagrams for basic and ultrabasic volcanic rocks through log-transformed ratios of high field strength elements and implications for petrogenetic processes. *Revista Mexicana de Ciencias Geológicas* **28**(1), 24–44.

Verma, S.K., Pandarinath, K., Verma, S.P. 2012. Statistical evaluation of tectonomagmatic discrimination diagrams for granitic rocks and proposal of new discriminant-function-based multi-dimensional diagrams for acid rocks. *International Geology Review* **54**(3), 325–347.

Verma, S.P. 2013. Application of 50 multi-dimensional discrimination diagrams and significance tests: deciphering compositional similarities and differences between Hawaiian and Icelandic volcanism. *International Geology Review* **55**(12), 1553–1572.

Verma, S.K., Verma, S.P. 2013. Identification of Archaean plate tectonic processes from multidimensional discrimination diagrams and probability calculations. *International Geology Review* **55**(2), 225–248.

Verma, S.P., Rivera-Gómez, M.A. 2013a. Computer programs for the classification and nomenclature of igneous rocks. *Episodes* **36**, 115–124.

Verma, S.P., Rivera-Gómez, M.A. 2013b. New computer program TecD for tectonomagmatic discrimination from discriminant function diagrams for basic and ultrabasic magmas and its application to ancient rocks. *Journal of Iberian Geology* **39**(1), 167–179.

Verma, S.P., Pandarinath, K., Verma, S.K., Agrawal, S. 2013. Fifteen new discriminant-function-based multi-dimensional robust diagrams for acid rocks and their application to Precambrian rocks. *Lithos* **168**, 113–123.

Winchester, J.A., **Floyd, P.A. 1976**. Geochemical magma type discrimination: application to altered and metamorphosed basic igneous rocks. *Earth and Planetary Science Letters* **28**(3), 459–469.

Winchester, J.A., **Floyd, P.A. 1977**. Geochemical discrimination of different magma series and their differentiation products using immobile elements. *Chemical Geology* **20**, 325–343.

Winkler, H. G. 1979. A key to determine metamorphic grades and major reaction-isograds or isograds in common rocks. In: *Petrogenesis of Metamorphic Rocks*, Klemke, P. (ed.). Springer: New York; 239–255.

Wise, W.S., **Eugster, H.P. 1974**. Celadonite: synthesis, thermal stability and occurrence. *American Mineralogist* **49**, l03l–1083.

Wood, D.A. 1980. The application of a Th-Hf-Ta diagram to problems of tectonomagmatic classification and to establishing the nature of crustal contamination of basaltic lavas of the British Tertiary Volcanic Province. *Earth and Planetary Science Letters* **50**(1), 11–30.

Yañez, P., **Ruiz, J.**, **Patchett, P.J.**, **Ortega-Gutiérrez, F.**, **Gehrels, G.E. 1991**. Isotopic studies of the Acatlán Complex, southern México: implications for Paleozoic North American tectonics. *Geological Society of America Bulletin* **103**, 817–828.

Zhou, Y., **Murphy, M.A.**, **Hamade, A. 2006**. Structural development of the Peregrina–Huizachal anticlinorium, Mexico. *Journal of Structural Geology* **28**(3), 494–507.

Ziegler, P.A. 1990. Collision related intra-plate compression deformations in Western and Central Europe. *Journal of Geodynamics* **11**(4), 357–388.

SUPPORTING INFORMATION

Additional supporting information may be found in the online version of this article at the publisher's web site.

Scientific editing by Brian McConnell